Application and verification of ECMWF products 2021

Hellenic National Meteorological Service (HNMS)
Dimitra Boucouvala, I.Kouroutzoglou and Ch. Kolyvas

1. <u>**Summary of major highlights**</u>

The ECMWF products are widely used in HNMS and are essential tools for our daily forecast.

The medium-range weather forecasts at the HNMS are based primarily on the deterministic ECMWF forecast. Both the 00 UTC and 12 UTC cycles of the ECMWF forecasts are received daily in the current resolution. For short-range forecasting and for observation of local characteristics of weather patterns in Greece, the output of the limited area models is used in conjunction with the ECMWF products.

Daily verification is performed for the surface fields of the IFS products as well as for the high-resolution limited area model (COSMO-GR at 4 and at 1km) that are used by the HNMS forecasters. Moreover, starting from MAM 2020 the verification of ICON at 2.5 km is also available. The relative performance of the models is subject to intercomparison.
.

2. <u>**Use and application of products**</u>

2.1   Direct use of ECMWF Products

The HNMS forecasting centre continues to use ECMWF products in conjunction with the products of its limited area models for the general 7-day forecast that is provided to the public as well as for the sea state forecast for the Eastern Mediterranean and, finally, the forecast for aeronautical purposes. The IFS forecast products are also consulted by the forecaster on duty and used to complete the awareness report for the European MeteoAlarm website.

The EPS products (plumes, meteograms, ensemble probability maps) are retrieved daily from the ECMWF website and are of particular value to the HNMS forecasters, especially the d+4 to d+7 forecast where the value of the deterministic forecasts is substantially reduced). An increasingly popular ECMWF product at the HNMS is the Extreme Forecast Index (EFI) for temperature and precipitation. As a measure of the distance from the climatological value (mean), the EFI maps are directly related to severe weather events. The monthly (and weekly) anomalies and seasonal forecasts are not used operationally but only for consultative or research purposes.

2.2   Other uses of ECMWF output

2.2.1 Post Processing

The HNMS implements a method for improving the temperature minimum and maximum forecast values for 50 locations in Greece (position of the stations) on a daily basis. This method uses a Kalman filtering technique, which is based on non-linear polynomials, incorporating all available quality-controlled observations in combination with the corresponding NWP data of the IFS model as well as from the limited area model COSMO-GR (4 and 1km). Application of the filter helps improve the temperature forecasts by eliminating possible systematic errors. The same technique is also used with the dew point temperature data (minimum and maximum) in order to correct biases related to relative humidity.

2.2.2 Derived fields

A wide range of derived fields are produced from the ECMWF model outputs (e.g. meteograms) for visualisation, issue of aeronautical forecasts and other applications at the forecasting center.

2.1.3 Modeling

ECMWF model output provides the lateral and boundary conditions for the execution of the daily simulations of the HNMS limited area model (COSMO-GR, WAM and ICON). As an option, ECMWF model output can also be used to provide the necessary input for the MOTHY air pollution trajectory model in the Eastern Mediterranean Sea (e.g. Daniel, 1996). The model provides the possible trajectories (locations) of oil (or floating objects) transport as well as the percentage of the oil spill that will reach the coast or the seabed.

Finally, the ECMWF deterministic model provides the necessary initial conditions to drive a wave forecast model (WAM) as an alternative option to COSMOGR. The wave forecast of the HNMS is based on the ECMWF version of the WAM (CYCLE 4) model. It is a third generation wave model which computes spectra of random short-crested wind-generated waves and is one of the most popular and well tested wave models. Verification of the calculated wave height and direction has been implemented with the use of observations taking by the buoys positioned around the Greek Seas (POSEIDON system).

3. Verification of ECMWF products

In order to determine the quality of the NWP products at the Hellenic National Meteorological Service (HNMS), a verification process is applied based on a tool that was developed through the **CO**nsortium for **S**mall-scale **MO**deling (COSMO). This operational conditional verification tool, known as **VER**ification **S**ystem **U**nified **S**urvey (VERSUS), the development of which was coordinated by the Italian Meteorological Service, is currently used by the HNMS for all verification activities concerning the weather forecast models. The operational verification system at the HNMS has been expanded to include verification of ensemble forecasts as well as wave model forecasts.

For research reasons and special test cases, the spatial verification methods software package VAST (VERSUS Additional Statistical Techniques), developed by the COSMO consortium offers a number of neighbourhood verification tools and is mainly used for precipitation (Gofa at al. 2018).

Monthly and seasonal verification is performed for the surface fields of the IFS products as well as for the high-resolution limited area model (COSMO-GR at 4, 1km and ICON at 2.5km) that are used by the HNMS forecasters.

3.1   Objective verification

3.1.1 Direct ECMWF model output

The forecasted values of weather parameters are compared with synoptic meteorological data from the HNMS operational network of stations and a range of statistical scores is calculated on a daily, monthly and yearly basis. The surface verification is performed by using the SYNOP data from the most reliable surface stations.

The continuous variables that are routinely verified are the 2m temperature, 2m dew point temperature, Mean Sea Level pressure,   10m wind speed and total cloud cover. For dichotomic parameters such as precipitation, the 6-, 12- and 24h-hour precipitation amounts are verified using indices from the respective contingency tables for the 72-hour forecast horizon. The thresholds for the precipitation amounts range from 0.2mm up to 30mm, accumulated in different time ranges. A selection of statistics for 12h is presented in the current report.

The RMSE and Bias scores are calculated for every forecast cycle, every 3 hours from the t+3 to the t+120 forecast hour (here presented up to 72h) for every synoptic station, indicating the degree to which the forecast values differ from the observations. The scores, which are averaged over all stations, are presented below. The verification was performed for every season (DJF19/20-SON20), ECMWF/IFS statistics are represented with the red lines. Our local models COSMOGR (4,1 km) and ICON (2.5 km resolution) are also depicted in the graphs. The main findings are as follows:
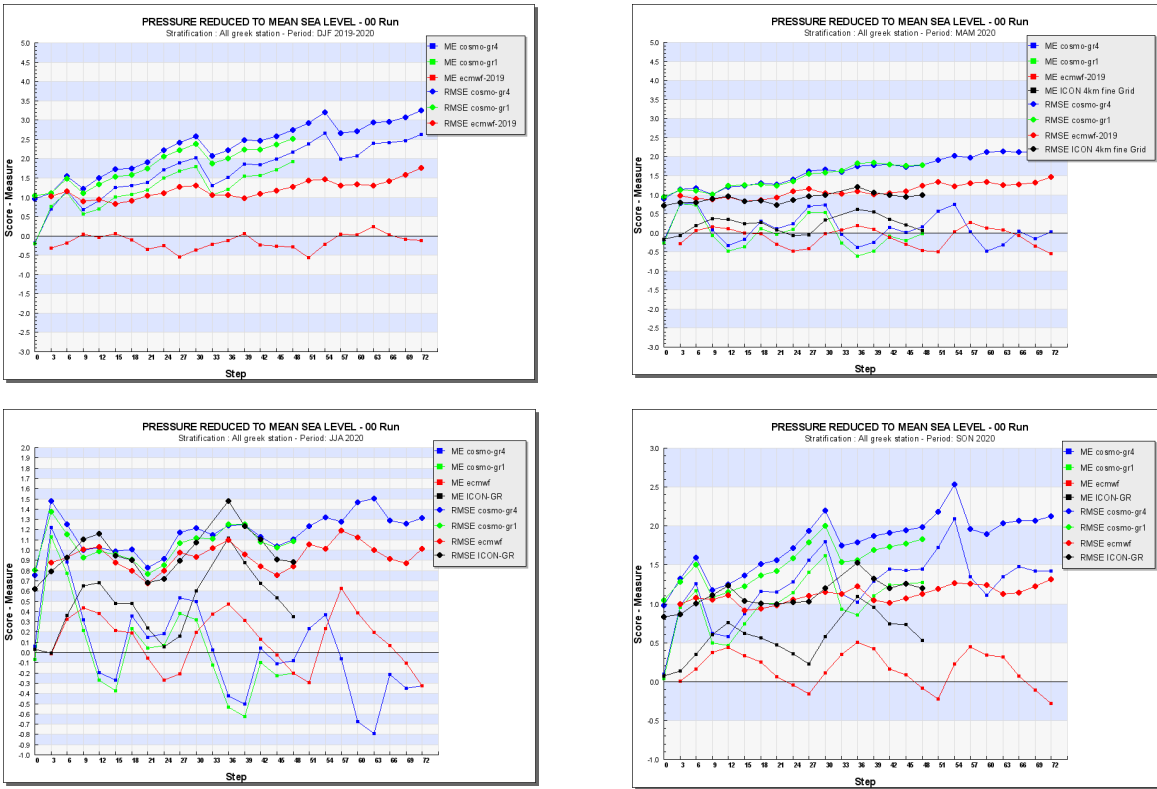
Fig. 1. RMSE and Bias (ME) score for MSLP from all models (00 UTC run) for DJF20 (left top), MAM20 (right top), JJA20 (left bottom) and SON20 (right bottom). Red lines show IFS-ECMWF model scores

Mean Sea Level Pressure: (Fig. 1) A slight propagation of the error (RMSE) with forecast time is evident for all seasons. RMSE IFS-ECMWF values are lower than other HNMS models. A diurnal RMSE variation with higher values in warm hours is shown in JJA. IFS-ECMWF bias values indicate a slight MSLP underestimation at night and overestimation in warm hours, mostly apparent in JJA and SON, in contrast to DJF and MAM, when bias diurnal variation is weak with values closer to zero.
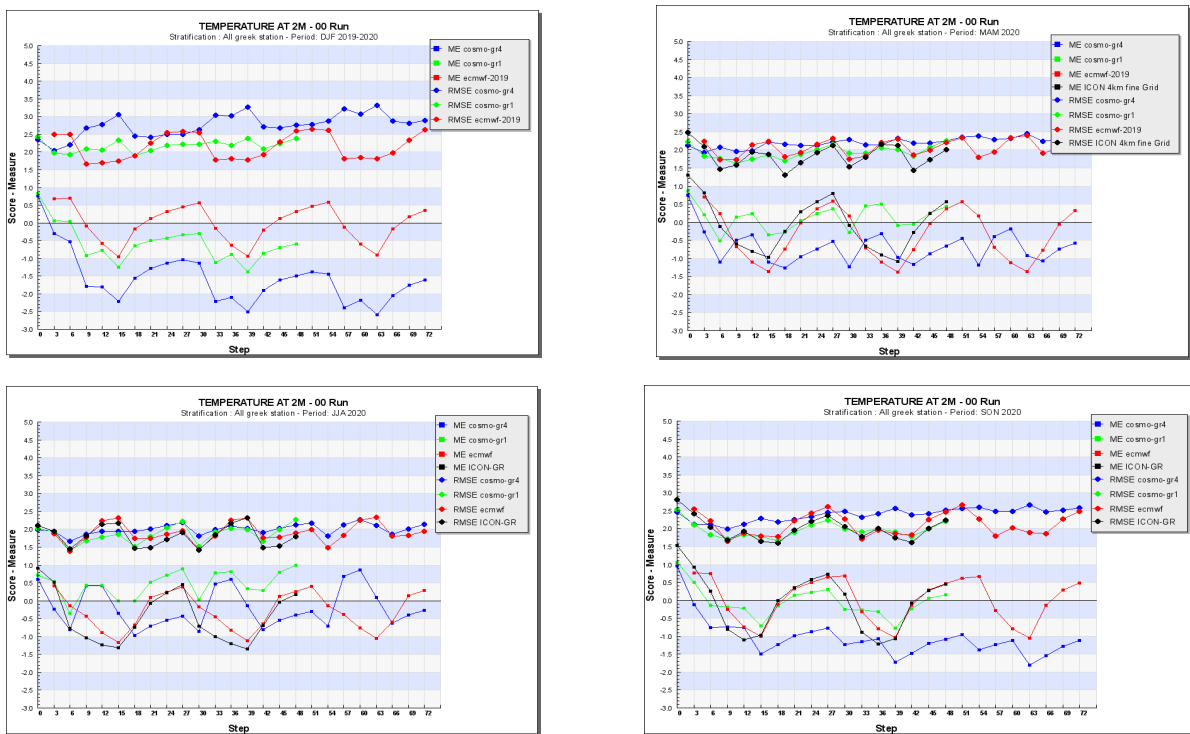
Fig.2 . Same as Fig.1 but for 2m Temperature

2m Temperature: A clear diurnal cycle of the Bias values is a characteristic of all seasons. (Fig. 2). IFS-ECMWF underpredicts the daytime temperature values to up to 1 K and slightly overpredicts nighttime values. Bias diurnal variation is similar to ICON2.5. RMSE also exhibits a weak diurnal variation with time with slightly higher values at night especially in DJF and SON. The average RMSE for all periods is approximately 2.5K and lower than COSMO models.
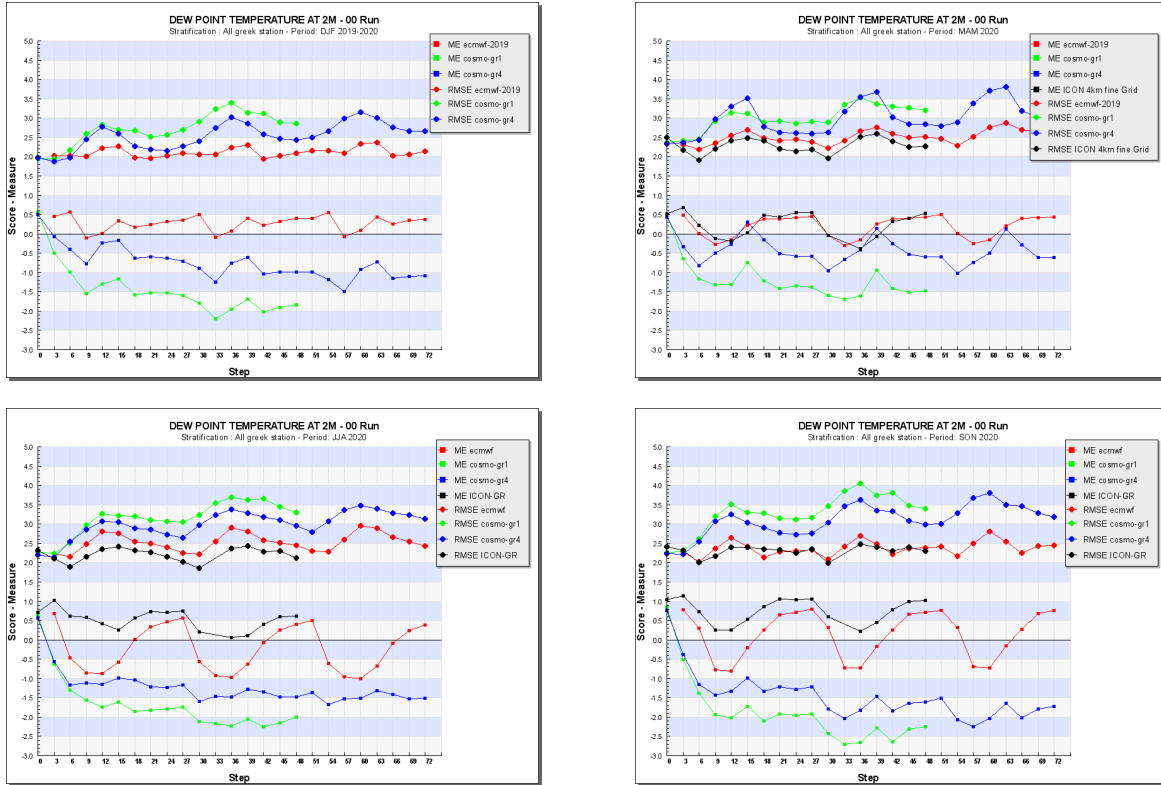
Fig.3   Same as Fig.1 but for 2m Dew Point Temperature

2m Dew Point Temperature*:* The diurnal cycle is evident in the Bias values especially in the summer and autumn DPT is underestimated the warm hours and overestimated at night. However, In DJF season, bias is almost zero. RMSE scores show a weak diurnal variability with higher values in the day, they are better than COSMO models and are more consistent with ICON2.5..
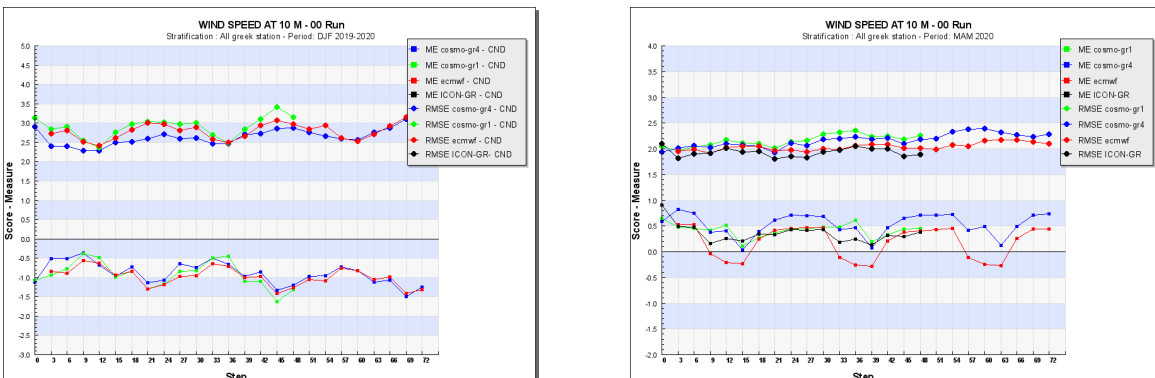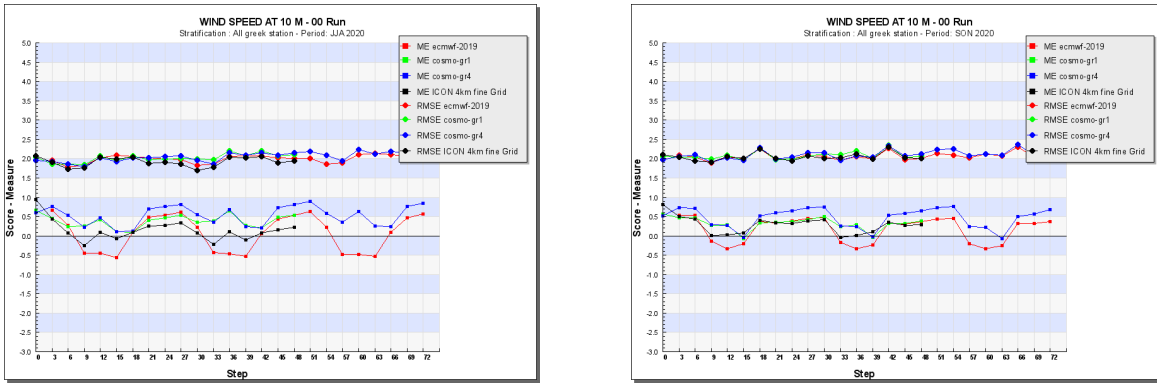
Fig.4   Same as Fig.1 but for 10m Wind Speed

10m Wind Speed: RMSE daily variation is weak and values are similar (around 2.5 m/sec) for all models Bias values for JJA show some underestimation of winds in warm hours and overestimation at night. (Fig. 4). In DJF season, there is a constant wind speed underestimation which increases with forecast time.
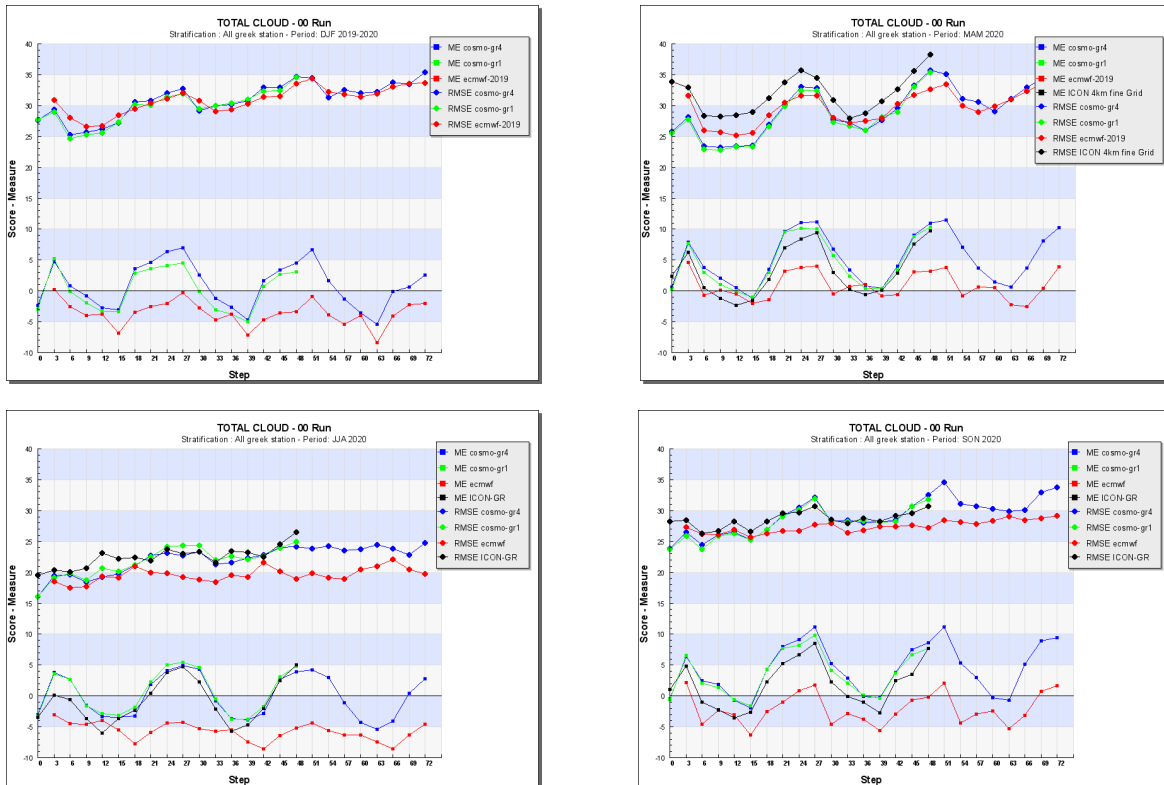
Fig.5   Same as Fig.1 but for Total Cloud Cover

Cloud Cover: A general slight underestimation of cloud cover percentage from IFS-ECMWF model is apparent in all seasons except spring as well as a relatively weak daily cycle of the bias. The RMSE values slightly increase with lead time with better performance during the summer season when weather conditions are more stable and cloud cover amount is low (Fig.5). The TCC RMSE scores of IFS-ECMWF are generally better than other forecast models especially in JJA and SON.

Precipitation:
Precipitation is commonly accepted as the most difficult weather parameter to correctly predict in terms of its spatial and temporal structure due to its stochastic behaviour. Verification is based on categorical scores that use contingency tables for specific thresholds. For this report, the most common categorical scores FBI (Bias), FAR (False Alarm Ratio) and POD (Probability of Detection).of 12h-hourly accumulated precipitation amounts are presented, for thresholds of 0.2,1,5,10mm (columns) for each season (rows).

GREECE

DJF	MAM	JJA	SON
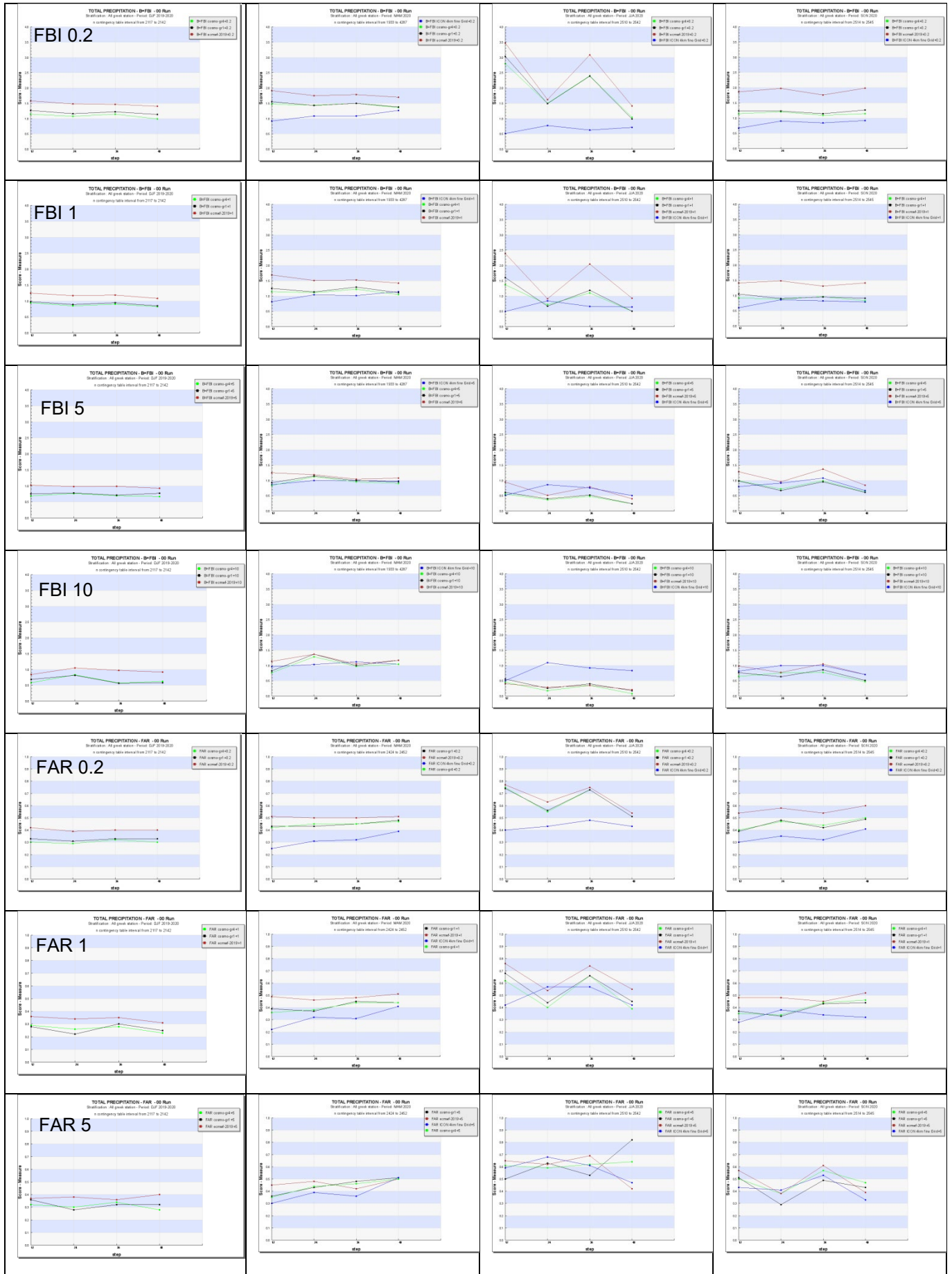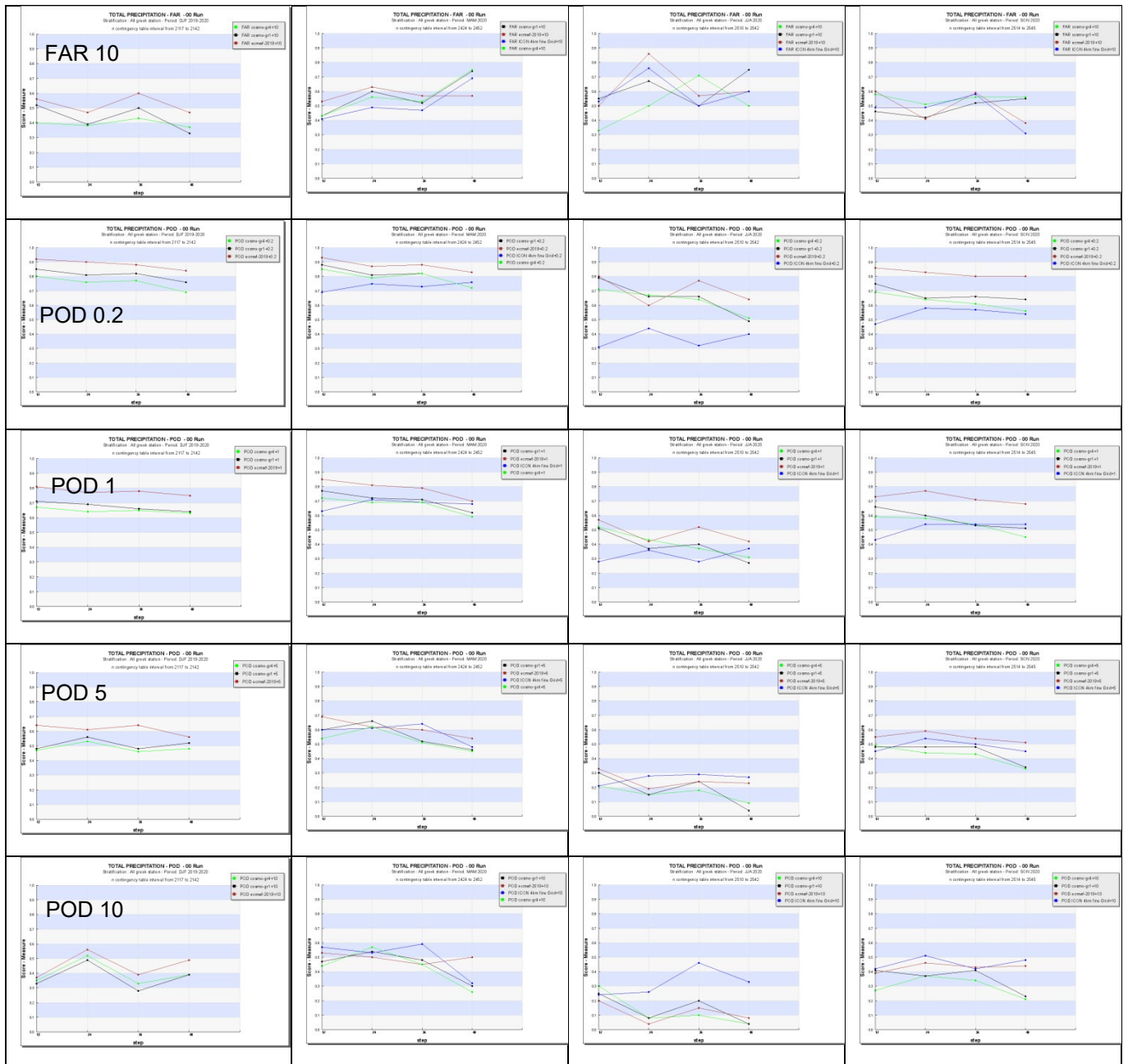
Fig.6 *Scores for 12h precipitation with forecast time (x axis): FBI, (rows 1-4) FAR (rows 5-8)and POD (rows 9-12) for threshold 0.2, 1, 5,10mm on each row on each score respectively for DJF, MAM, JJA, SON (columns from left to right. Red line represents IFS-ECMWF*

FBI: Overestimation of precipitation events (larger for 00-12h) for low thresholds, with a clear diurnal cycle in warm seasons especially JJA, more than the other forecast models. For higher thresholds, there is a slight underestimation of events and a weaker diurnal cycle and FBI values are comparable to other models.

FAR: Diurnal cycle in warm seasons especially in JJA with higher values for 00-12h especially for low thresholds. No significant difference of FAR values with increasing threshold and forecast time. Less false alarms are in DJF where no diurnal cycle is apparent. FAR values are slightly higher than other models.

POD: Higher POD in DJF and lower in JJA. POD values drop with increasing threshold and forecast time. POD values for IFS-ECMWF are higher than other models.

3.2   Subjective verification (by I. Kouroutzoglou)

3.2.1 Subjective scores (including evaluation of confidence indices when available)

3.2.2 Case studies

In general, systematic errors experienced by HNMS staff:

a) Underestimating of precipitation totals over Eastern –windward parts of Greece:

      i. when the 500 hPa prevailing flow is SW, or

      ii. a cold front crosses the country from the west and mainly SW, considering that the orography of continental Greece distorts the thermodynamic structure of the low level frontal activity

      iii. Extensive low level baroclinic zones without necessarily be combined to organized frontal activities, mainly from Northern Africa,

  b) On the contrary, overestimating of precipitation totals snowfall, in particular over NE mainland Greece,

  c) Often unsuccessful tracking of the movement of extensive, quasi-stationary cut-off lows (500hPa), located over a wide area in the Central - Eastern Mediterranean - secondary upper level cyclogenesis. For example when a warm upper level anticyclone forms in the Atlantic or the Western European area and upper level downstream development rejuvenates the pre-existed quasi-stationary cut-off low under the effect of a mobile polar front jet streak and the strengthening of the respective transverse ageostrophic circulations,

  d) Unsuccessful simulation of diabatic heating in the form of surface sensible and latent heat fluxes from the sea during the transitional time periods between warm and cold sea,

  e) Unsuccessful simulation of the transformations of surface frontal activities in cases where the absence of organized conveyor belts and wind component perpendicular to the frontal activities does not allow the surface depression to follow the typical life cycle of a mid-latitude surface depression from the incipient to the mature stage, for example the typical life cycle described in Shapiro and Keyser (1990). In these cases the dissipation of the cyclone's warm front and the formation of comma clouds or occluded fronts with persistence over a specific area, being steered by a stationary or quasi-stationary upper level cyclone, lead to problematic forecasts of the surface front's movement,

f) The general synoptic behavior of June and July 2020 over the Mediterranean area presenting resemblance with the respective period of 2018, allows us to expand the comment of paragraph (d) for the period of cold sea, as well. The increased frequency of establishment of upper level blocking anticyclones in the Atlantic or Western Europe and the resultant shift of the atmospheric circulation from zonal to meridional, allowed the southward propagation of upper level deep cyclonic circulations (often detected even in the 850hPa isobaric level) towards the southern parts of Mediterranean area, including the Eastern Mediterranean and Greece. Despite the fact that climatologically the air-sea interaction does not favor instability over the Eastern Mediterranean Sea surface during summer, lighting activity and thunderstorms were observed over the Ionian and the Aegean Sea during the above mentioned episodes between June and July 2020, implying that upper level dynamic forcing managed to overcome the tendency of a stable low level stratification over the sea surface. In the majority of these cases the ECMWF forecast precipitation failed to simulate effectively the cloudiness and the precipitation amounts over the sea and especially over the southern parts of the Aegean and Ionian Seas. Nevertheless, it is also a question whether the sign of the heat fluxes from the sea is reversed (from negative – instability to positive – stability), except the influence of the above mentioned upper level forcing. Although the air-sea interaction does not favor climatologically the instability over the Eastern Mediterranean Sea during summer, this does not mean that in any synoptic type Tair – Tsea >0. For example, in cases of surface and low level NW flow over Greece (existence of surface cyclogenesis and probably frontogenesis over the Eastern Europe and the Black Sea), the temperature of the surface air mass advected from the Eastern Balkans

towards the Aegean Sea will probably be smaller than the SST over the Aegean Sea (especially during the night hours). In these cases both the upper level dynamic processes and the respective surface and low level diabatic ones, will positively operate in order to have ω < 0 over the sea surface and the combination of potential and convective instability.

A case of particular interest including the main aspects of the above mentioned comments is the Mediterranean tropical-like cyclone of 17-20 September 2020 in Central Mediterranean affecting Greece which extremely strong weather phenomena. The cyclone was initially formed over the Gulf of Syrte during the time period between 14-15 September 2020, while according to the thermodynamic analysis made by the HNMS, including the calculation of the parameters determining the thermal symmetry and the warm core structure in both the upper the lower troposphere (Hart et al. 2003, Pytharoulis et al. 2018), during the period between 16-18 September 2020, the cyclone presented characteristics of a symmetric deep warm core structure during its E-NE propagation towards the Southern Ionian Sea and the western parts of Peloponnese. Despite the expected forecast adjustments of the cyclone strength and propagation while approaching the episode, the ECMWF operational model runs failed to effectively simulate the precipitation amounts, not in the area affected by the cyclone track (namely the southern parts of Greece, but in Central Greece and specifically over the region of Thessaly, where catastrophic flash floods and human casualties occurred. The above area, although located to the north of the vortex path, seemed to be affected by the strong low level convergence of warm and moist air masses with significant θe and θw anomalies advected over the eastern continental parts of Central Greece, under the induced low level S-SE flow, with the pre-existed relatively colder air masses, while the topography of the region reinforced the strong upward motions.

Despite the fact that this synoptic situation was affected by the formation and the evolution of a syb-synoptic vortex with individual thermodynamic characteristics and structure increasing the forecast uncertainty, one should probably waiting a more sufficient simulation of the kinematic characteristics and the deepening rates of the cyclone, for example 3 or 4 days before the initiation of the phenomenon. Nevertheless, the operational HRES ECMWF model presented differences between the successive runs until the 17th of September.
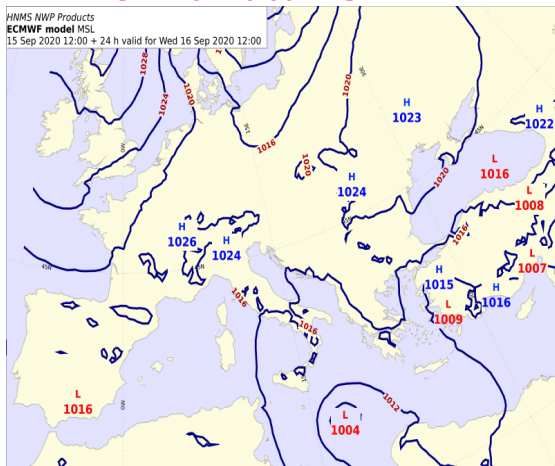
MSLP for 16/09 12UTC   **MSLP for 17/09 00UTC**
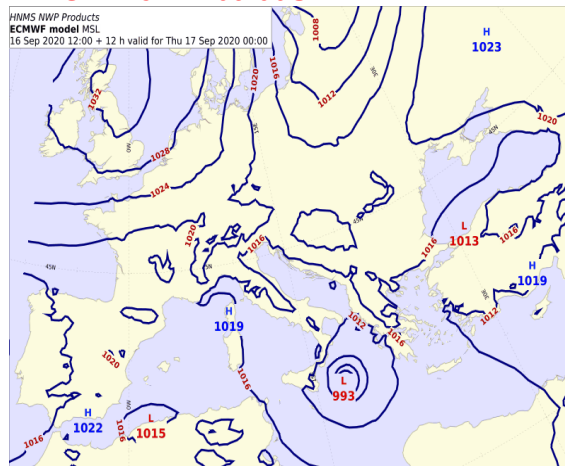
MSLP for 17/09 12UTC   **MSLP for 18/09 00UTC**
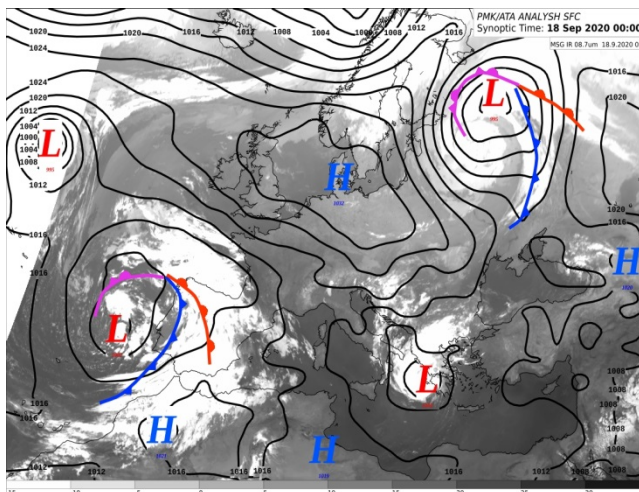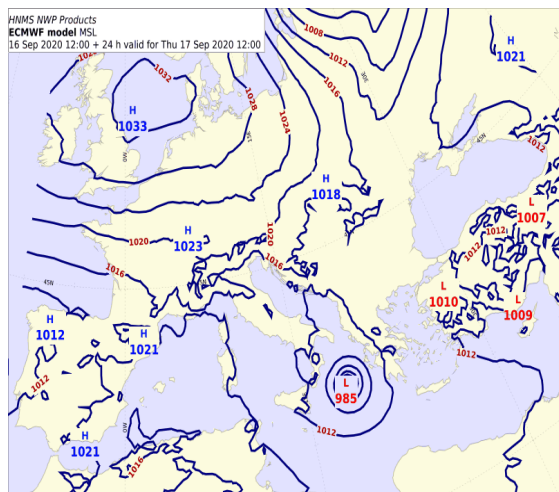
850hPa GH-T for 16/09 12UTC
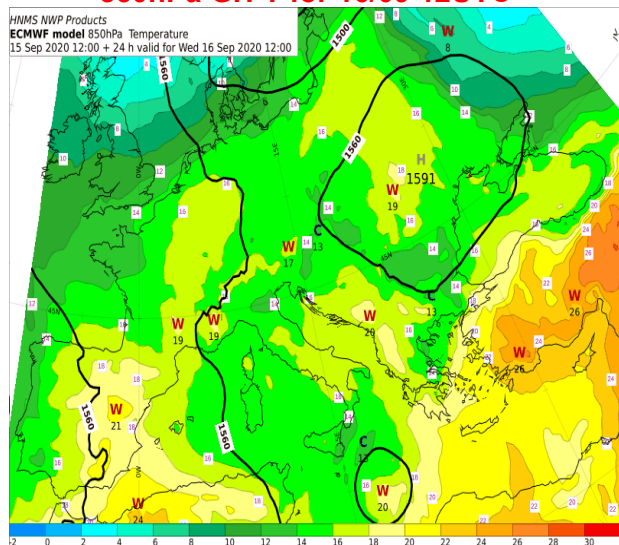
850hPa GH-T for 17/09 00UTC
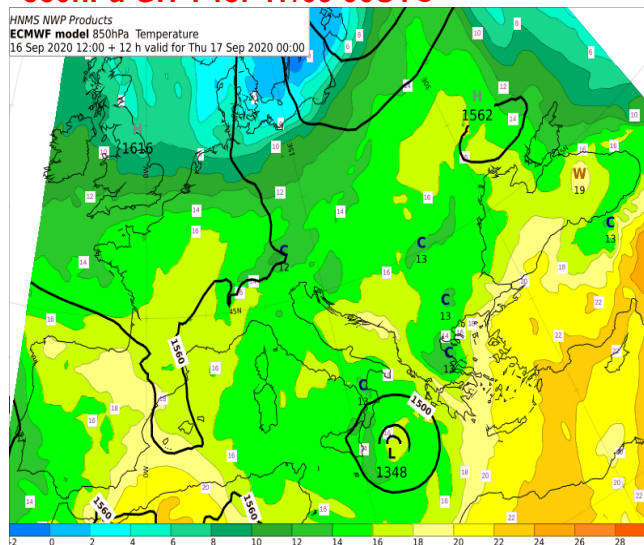
850hPa GH-T for 17/12UTC

850hPa GH-T for 18/00UTC
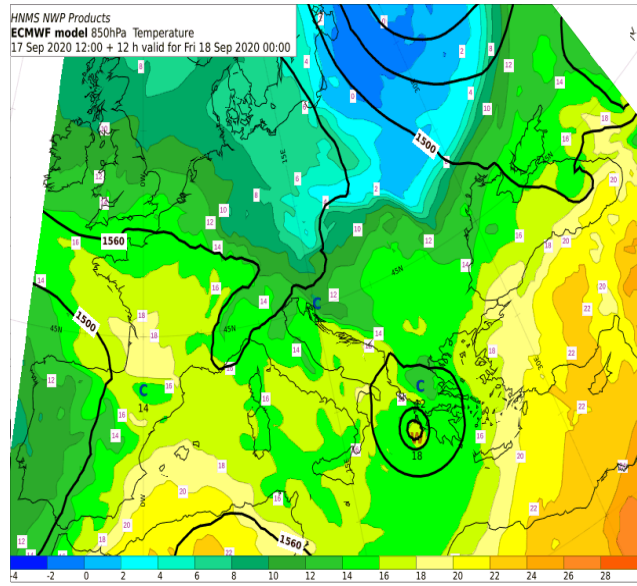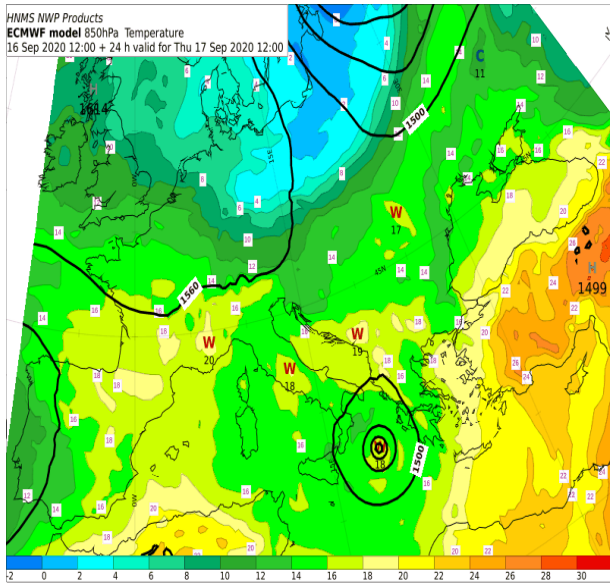
300hPa winds for 16/12UTC
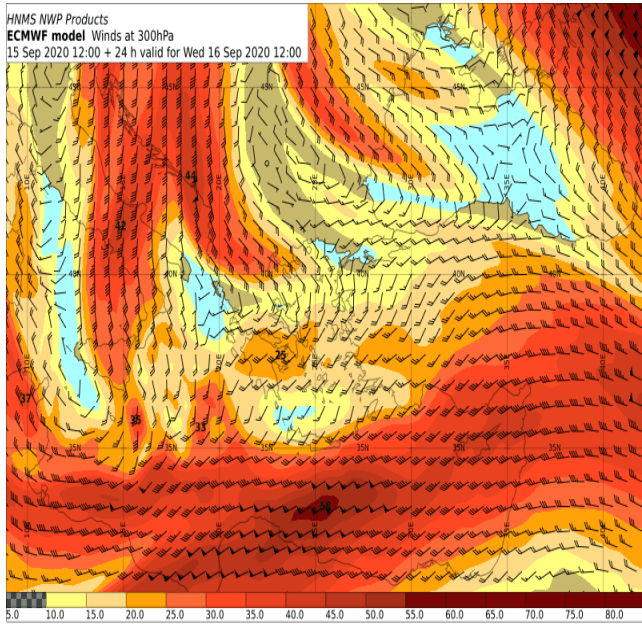
300hPa winds for 17/00UTC
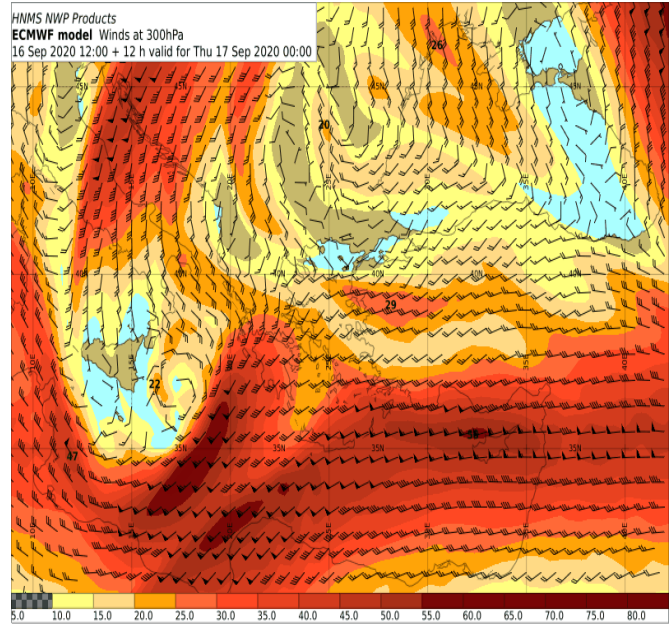
300hPa winds for 17/12 00UTC

HNMS NWP Products
ECMWF model Winds at 300hPa
16 Sep 2020 12:00 + 24 h valid for Thu 17 Sep 2020 12:00
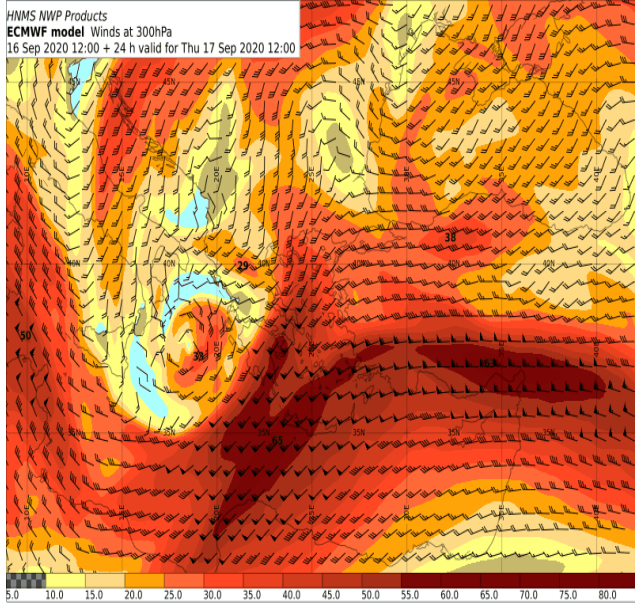
300hPa winds for 18/00UTC

HNMS NWP Products
ECMWF model Winds at 300hPa
17 Sep 2020 12:00 + 12 h valid for Fri 18 Sep 2020 00:00

500hPa GH-T for 16/12UTC

HNMS NWP Products
ECMWF model 500hPa GH + Temperature
15 Sep 2020 12:00 + 24 h valid for Wed 16 Sep 2020 12:00

500hPa GH-T for 17/00UTC

HNMS NWP Products
ECMWF model 500hPa GH + Temperature
16 Sep 2020 12:00 + 24 h valid for Thu 17 Sep 2020 12:00

500hPa GH-T for 18/00UTC

HNMS NWP Products
ECMWF model 500hPa GH + Temperature
17 Sep 2020 12:00 + 12 h valid for Fri 18 Sep 2020 00:00
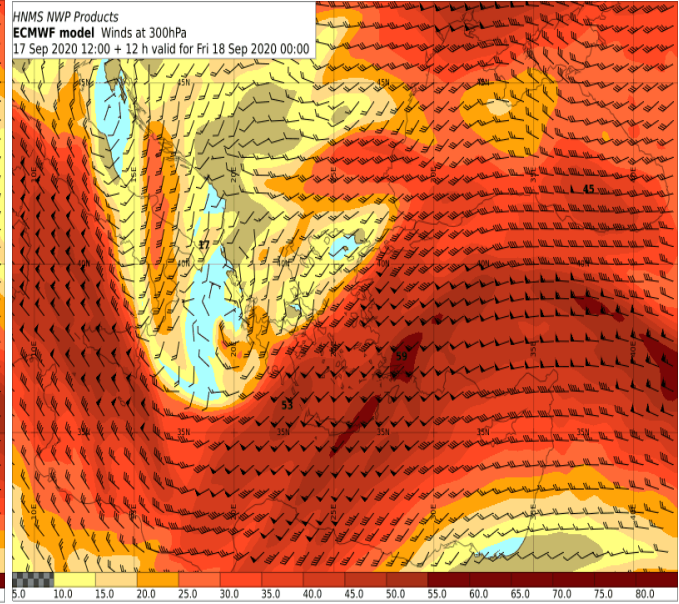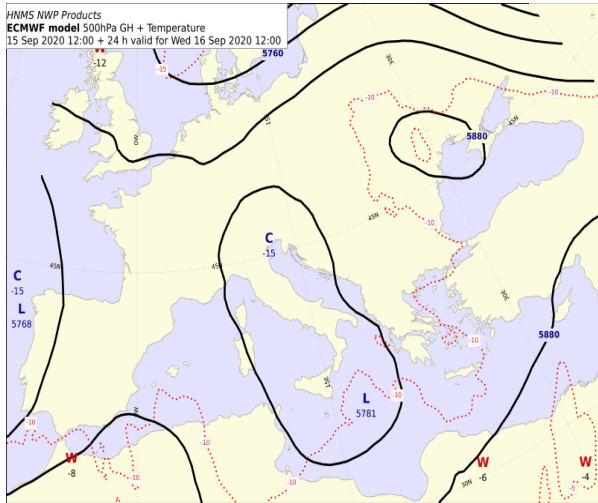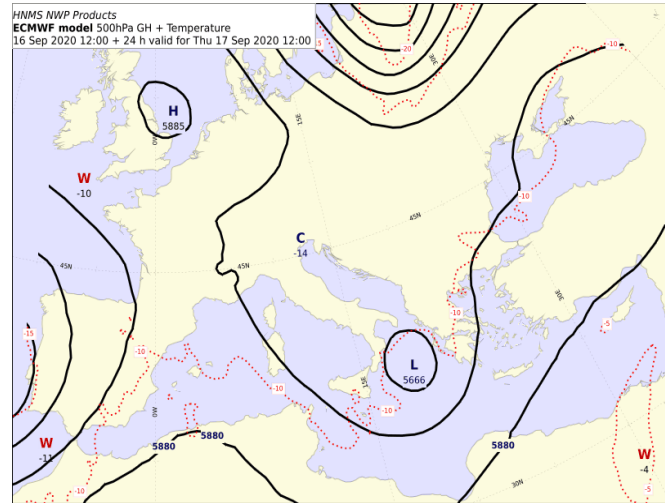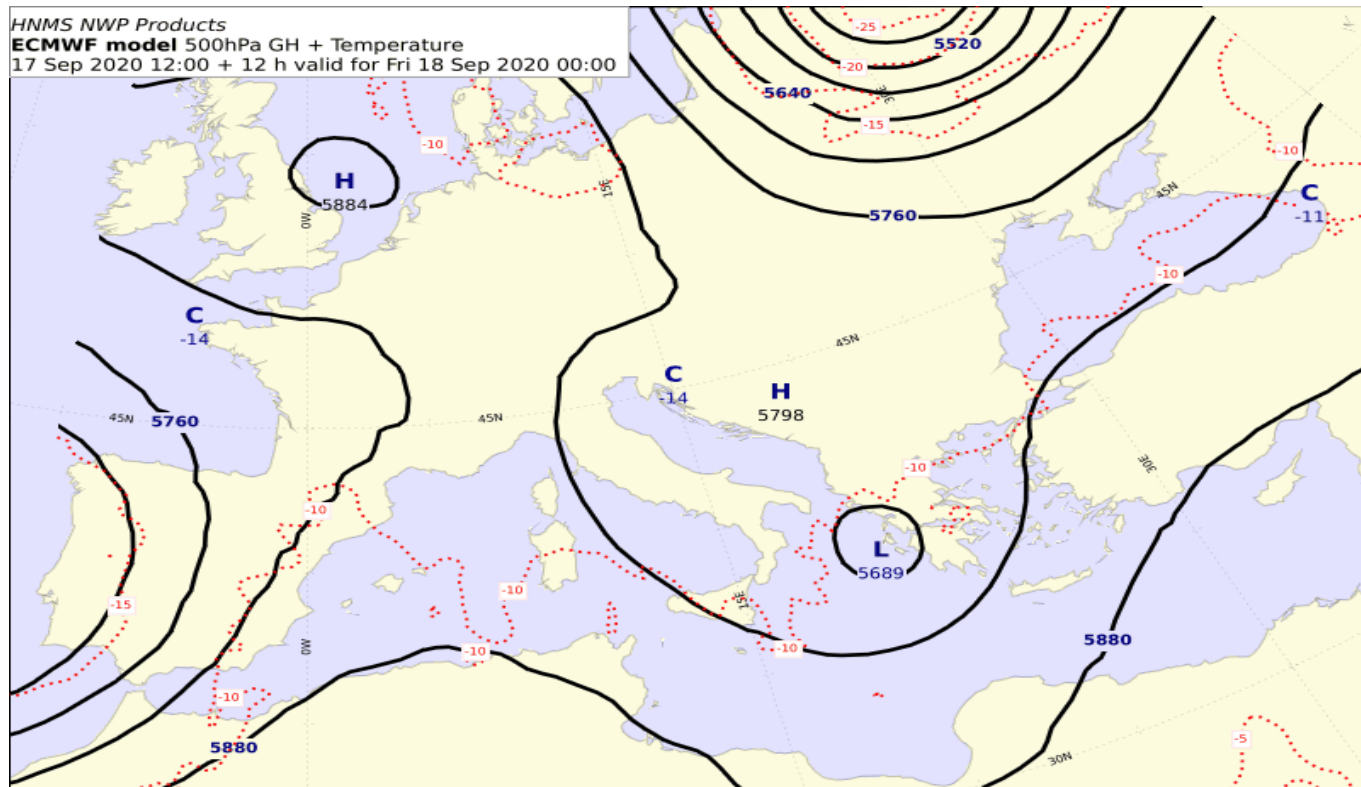
MSG IR IMAGE for 16/08:45UTC
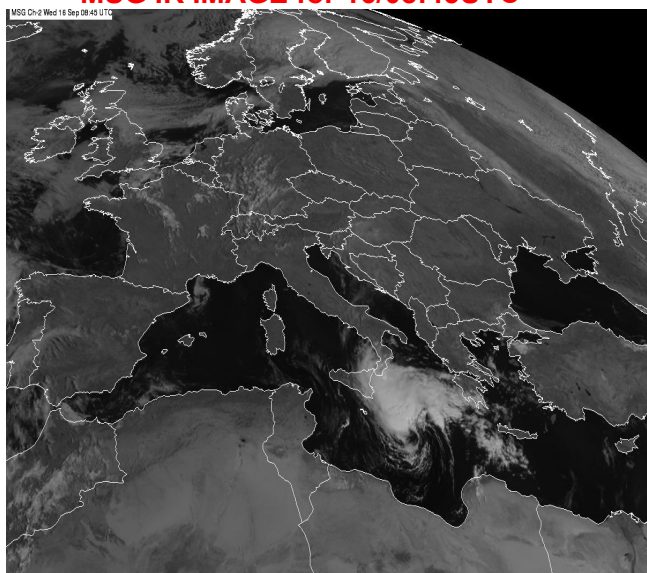
MSG IR IMAGE for 16/20:45UTC

13
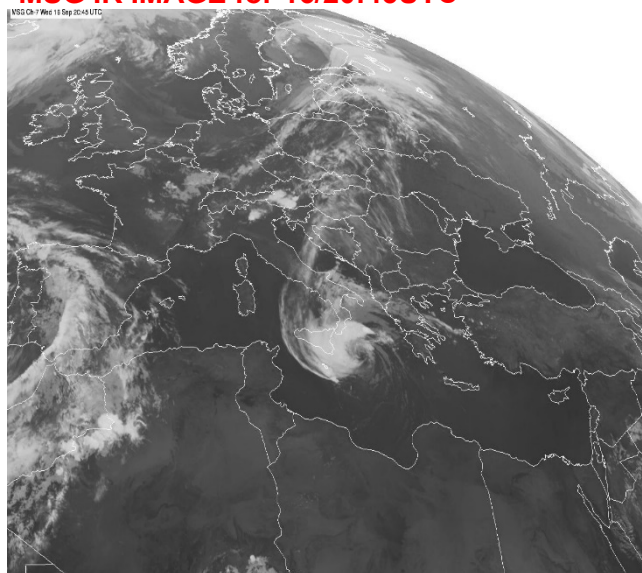
GREECE

MSG IR IMAGE for 17/08:45UTC
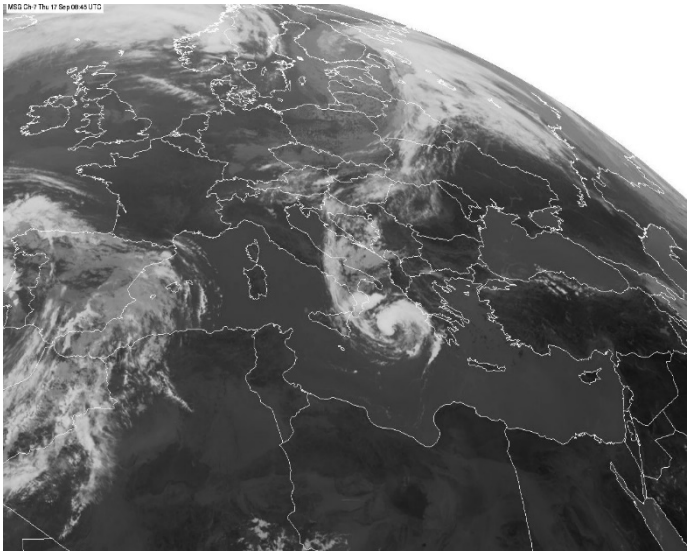
MSG IR IMAGE for 17/18:45UTC
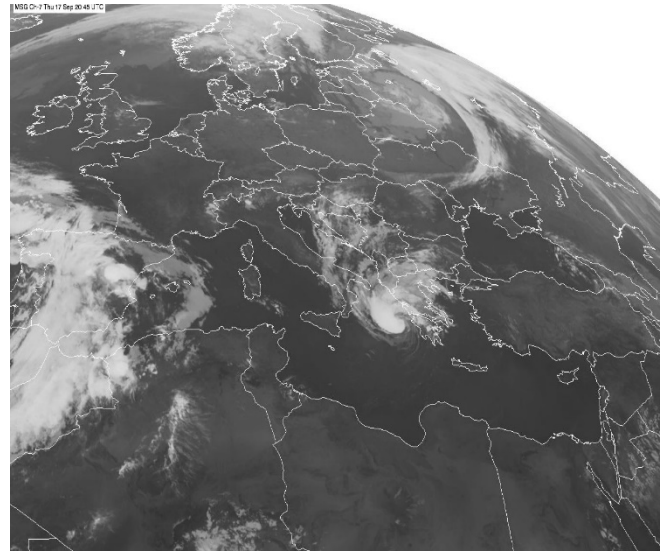
MSG IR IMAGE FOR 18/0845UTC
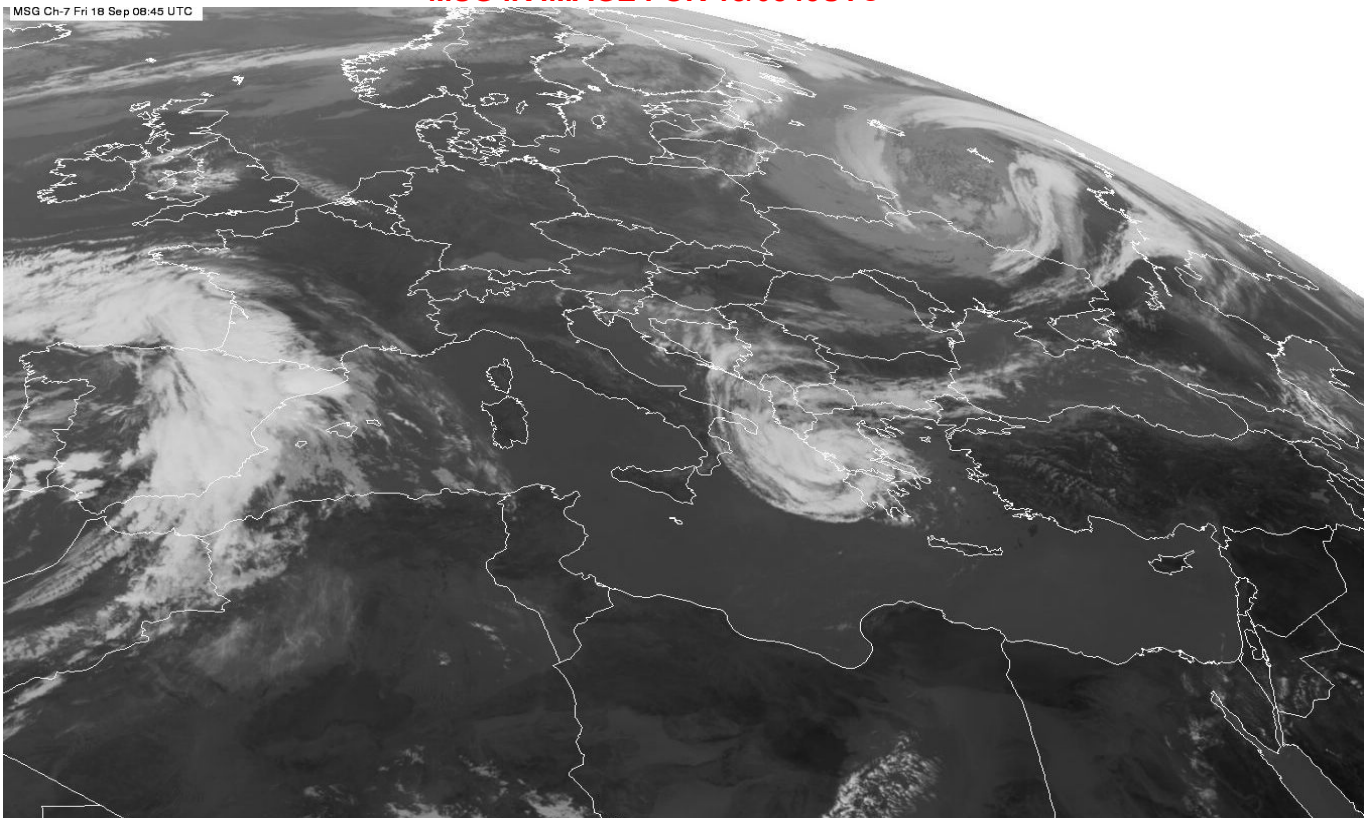
REAL TIME WEATHER FOR 17/09:20UTC   LIGHTNING ACTIVITY FOR 18/09UTC

14
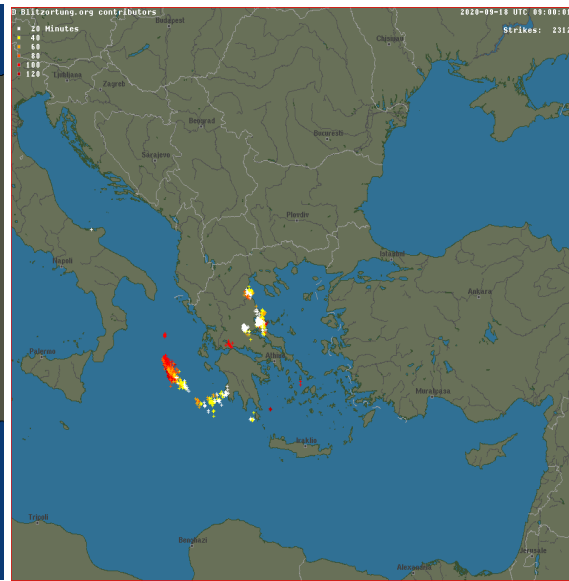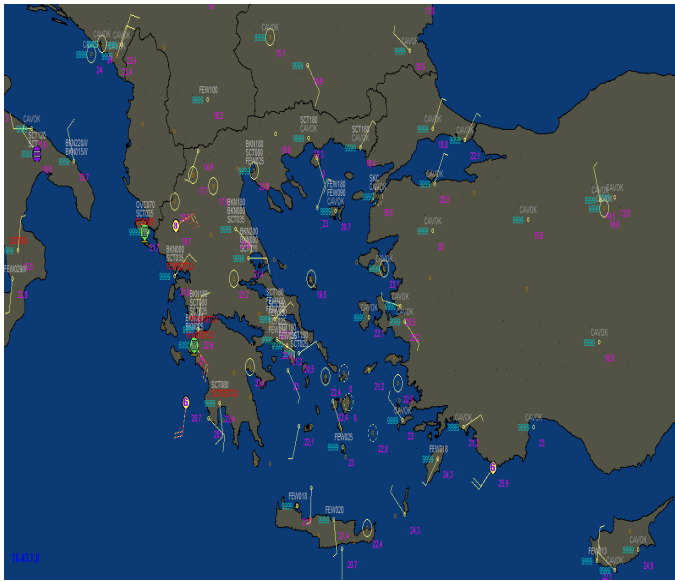
LIGHTNING ACTIVITY FOR 18/12UTC

LIGHTNING ACTIVITY FOR 18/15UTC
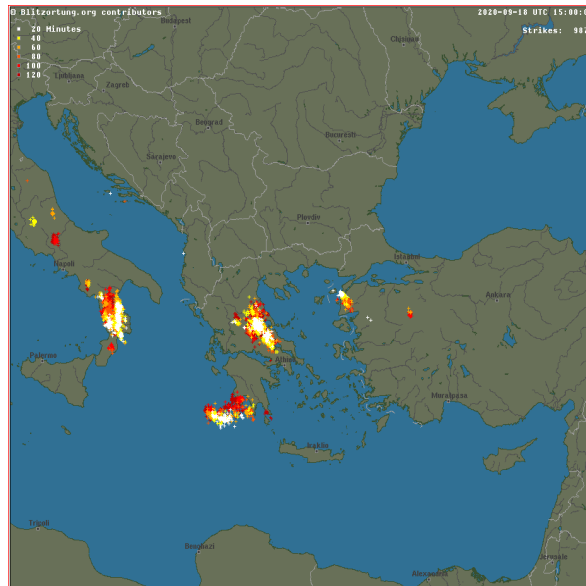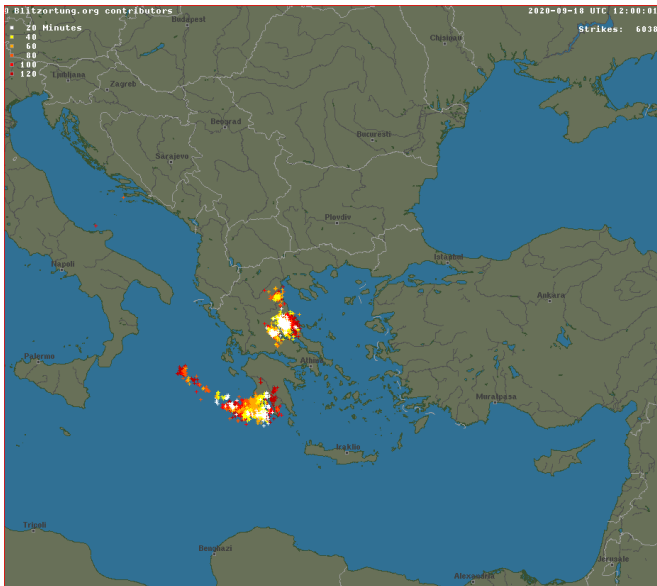
LIGHTNING ACTIVITY FOR 18/18UTC

LIGHTNING ACTIVITY FOR 18/23:10UTC

GREECE

\
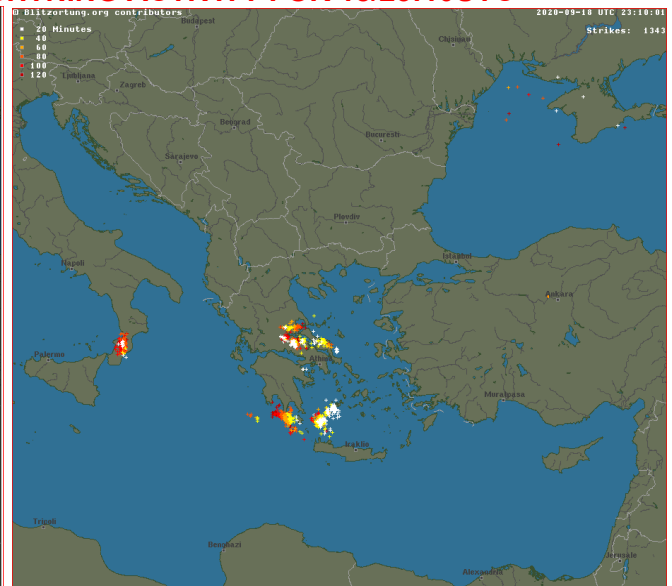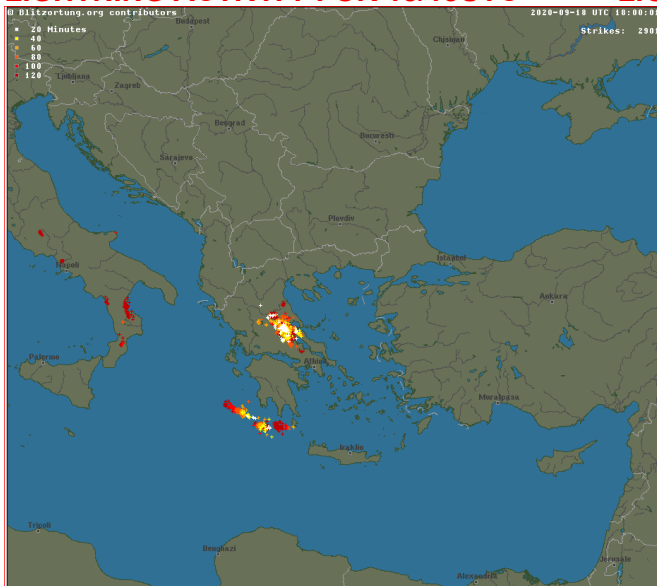
A second extremely significant synoptic case for the Eastern Mediterranean in general and the Greek region particularly was the case of 7-9 August 2020, with extremely strong flash floods and human casualties over the Euboea island specifically and the eastern continental parts of Central Greece in general. Considering that the displacement of the sub-tropical jet stream towards northern latitudes during summer does not usually allow vertically well-organized cyclonic circulations to be formed over the Mediterranean, in that case a deep cyclonic disturbance, vertically organized up to the 850hPa isobaric level, was formed on the eastern flanks of an upper level blocking anticyclone operating as dynamically unstable ridge (Prezerakos and Flocas 1996) providing favorable conditions form strong baroclinic instability. Although the ECMWF operational forecasts successfully simulated the synergistic way that convection and potential instability acted over the Ionian and the Aegean seas, the forecasted simulation failed to capture the magnitude of the low level convergence, with the strong low level N-NE flow advecting relatively cold air masses over an area where low level baroclinic processes favored the respective advection of warm and moist air from the southern Aegean Sea. The forecasted upper level 315K PV values along with the 2PVU potential temperature distributions (Hoskins and Berrisford 1988) strongly implied a tropopause folding and stratospheric intrusion over the area, with characteristics similar to those of a cyclonic system during winter. Nevertheless, it was the effect of the topography that seemed to be underestimated in this case, too.

300hPa WINDS for 07/00UTC   **300hPa WINDS for 07/12UTC**
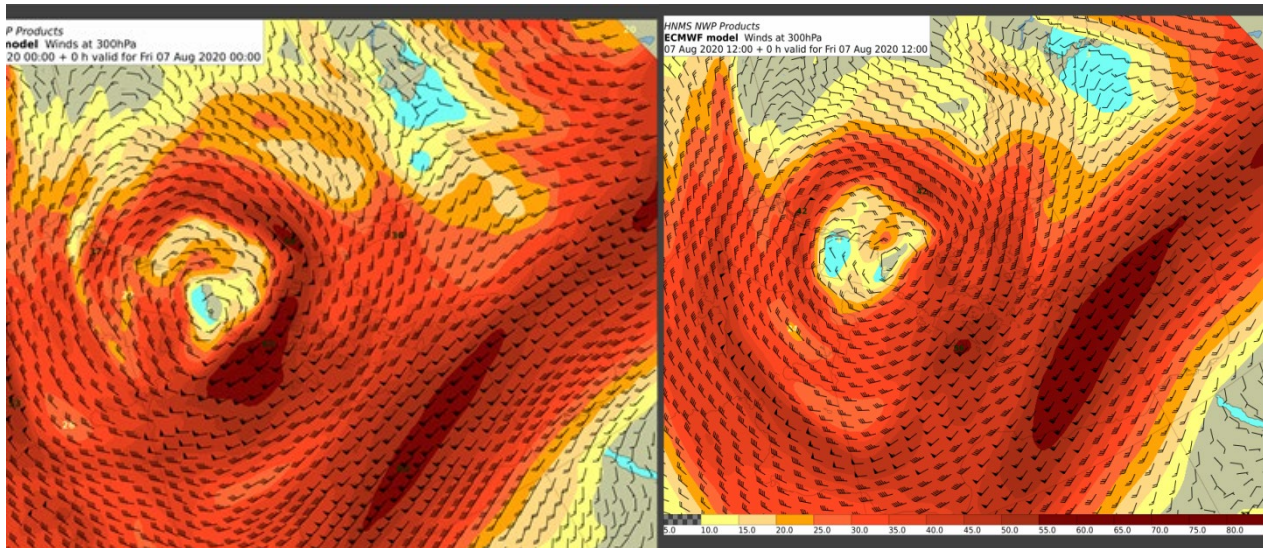
300hPa WINDS for 08/00UTC

300hPa WINDS for 08/12UTC
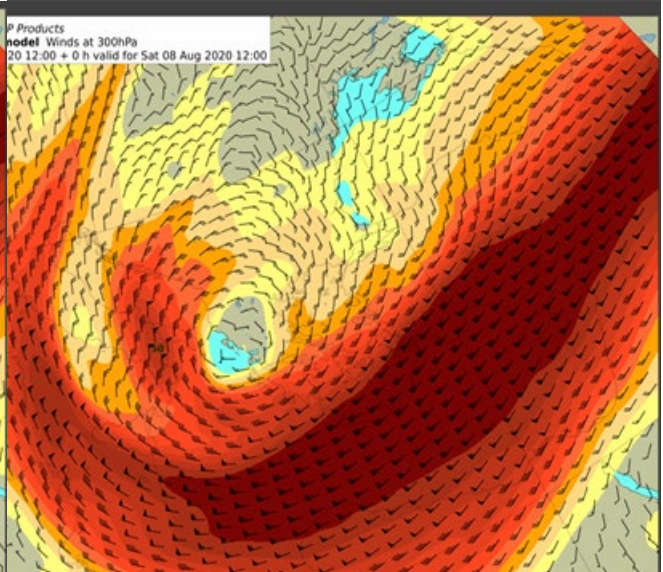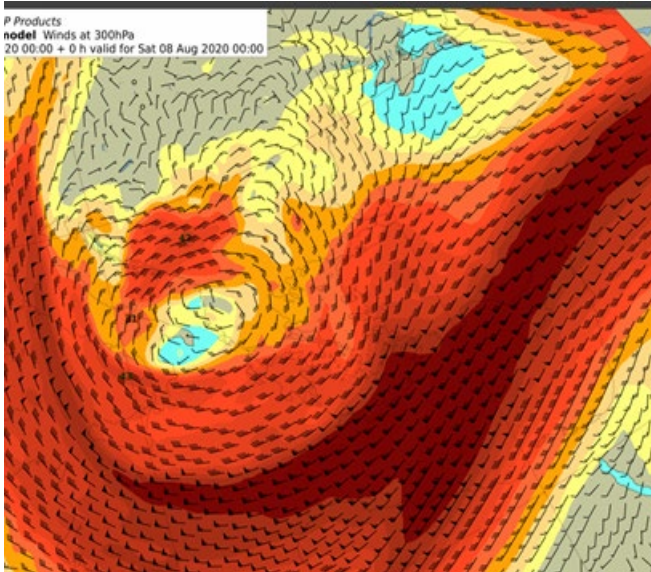
300hPa WIND for 09/00UTC
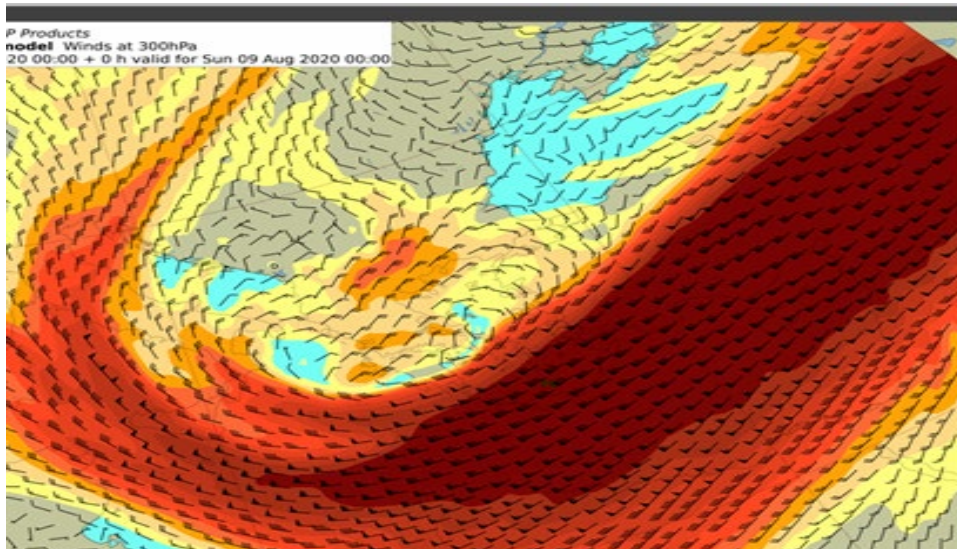
500hPa GH-T for 07/00UTC
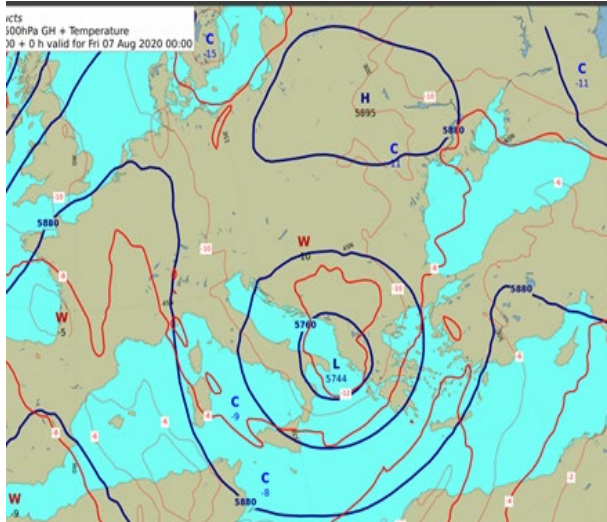
500hPa GH-T for 07/12UTC
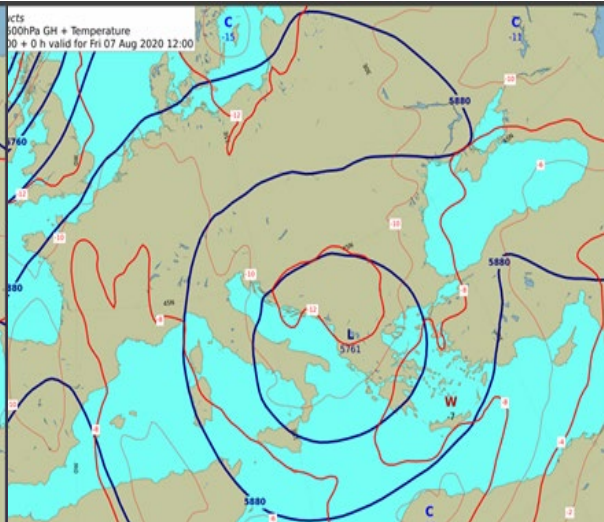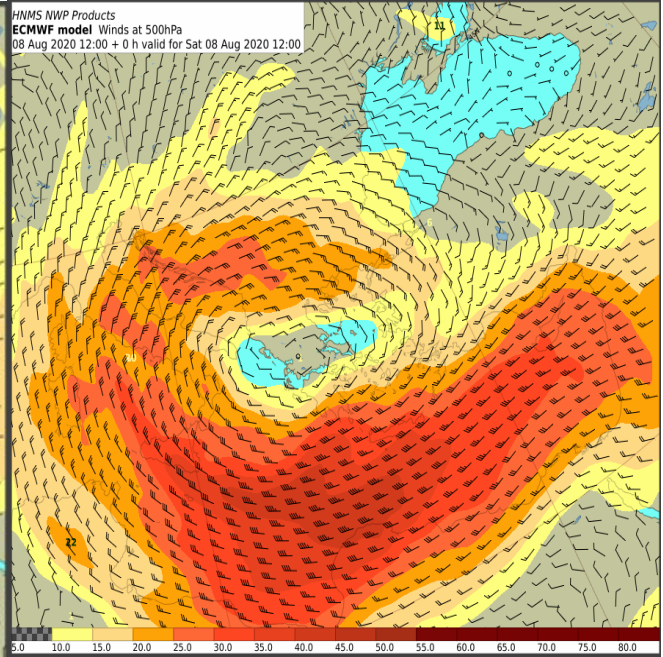

500hPa WINDS for 07/00UTC
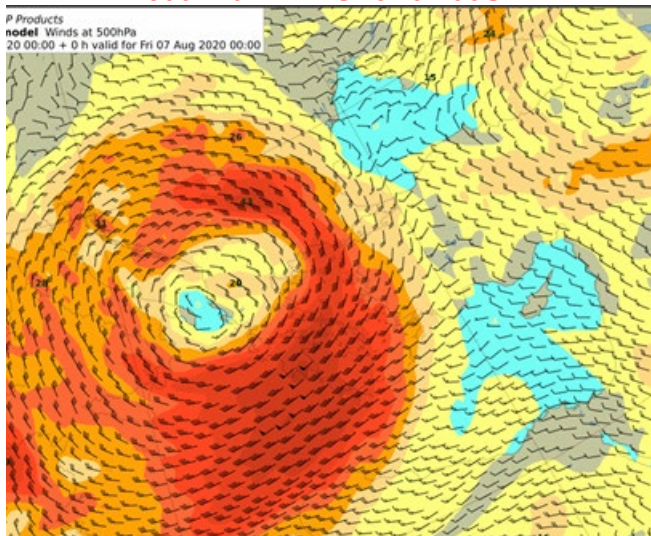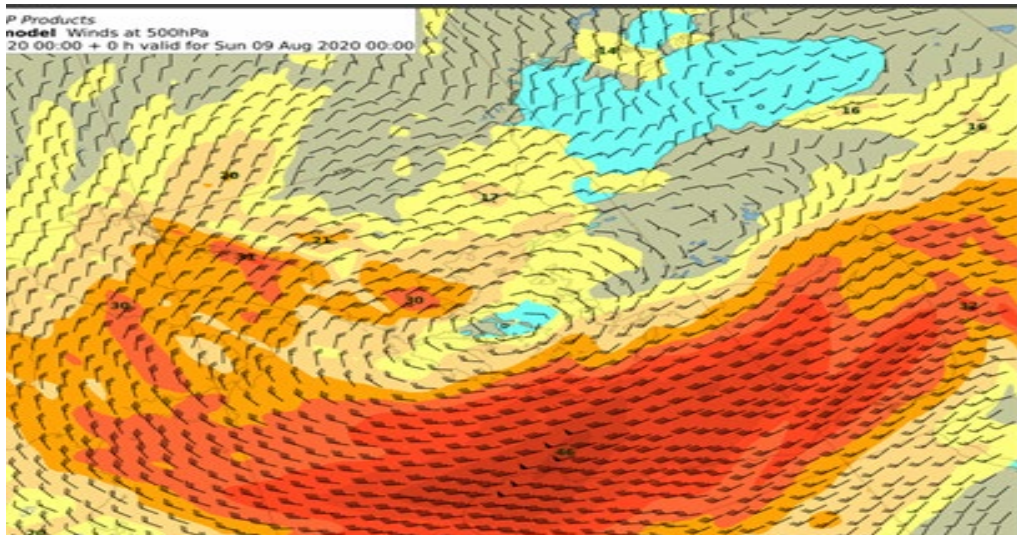
500hPa WINDS for 07/12UTC
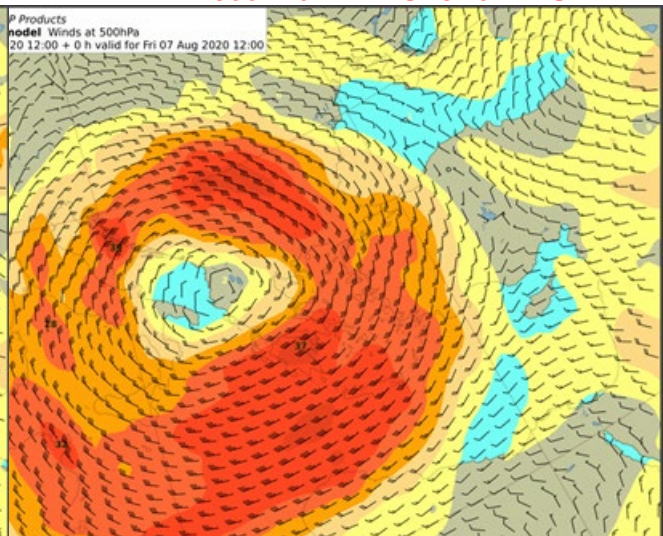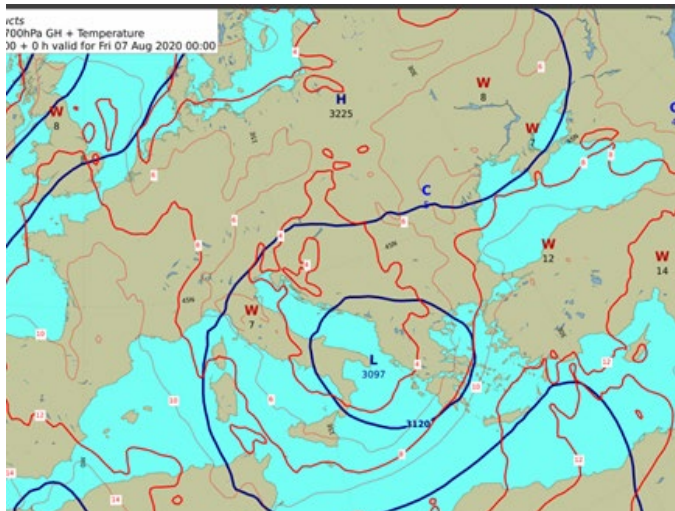
500hPa WINDS for 08/00UTC
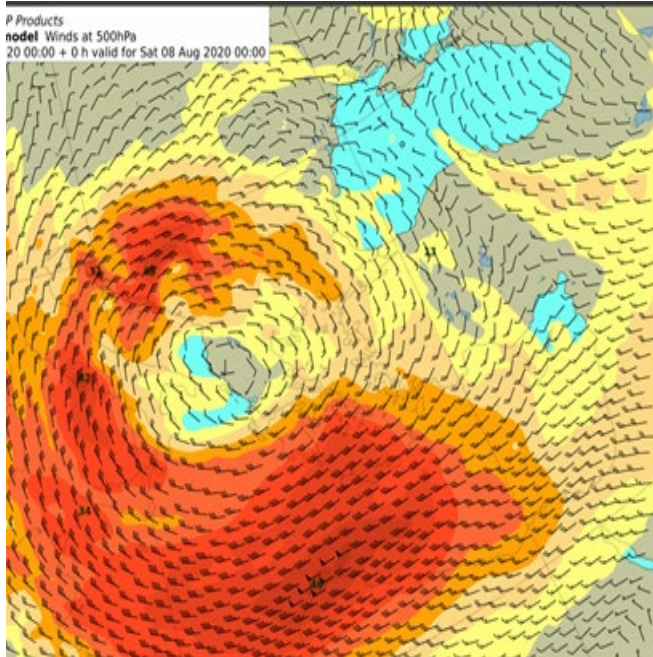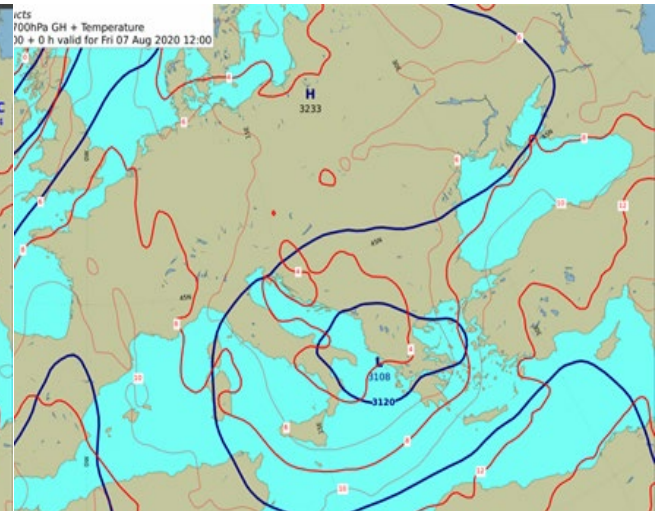
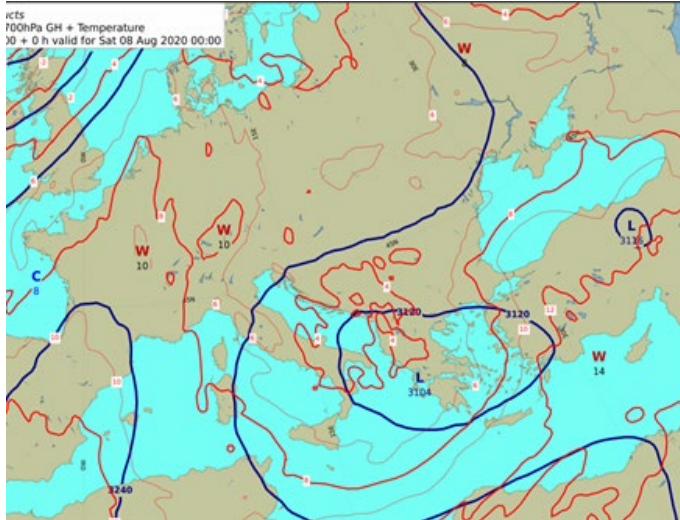**500hPa WINDS for 08/12UTC**

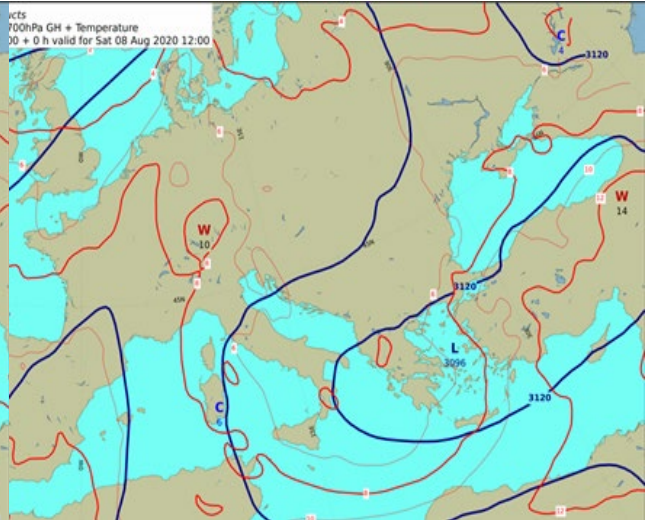**500hPa WINDS for 09/00UTC**

850hPa GH-T for 07/00UTC
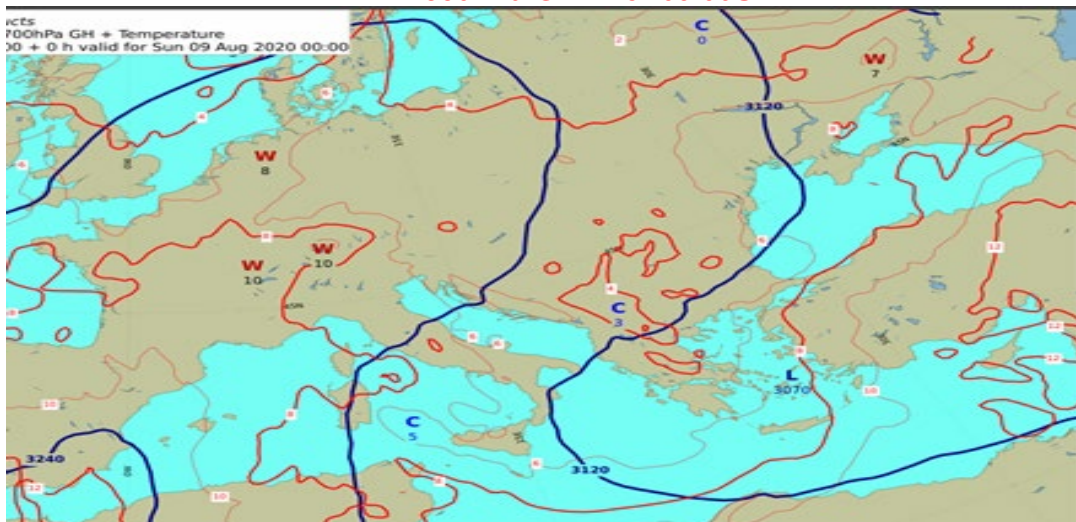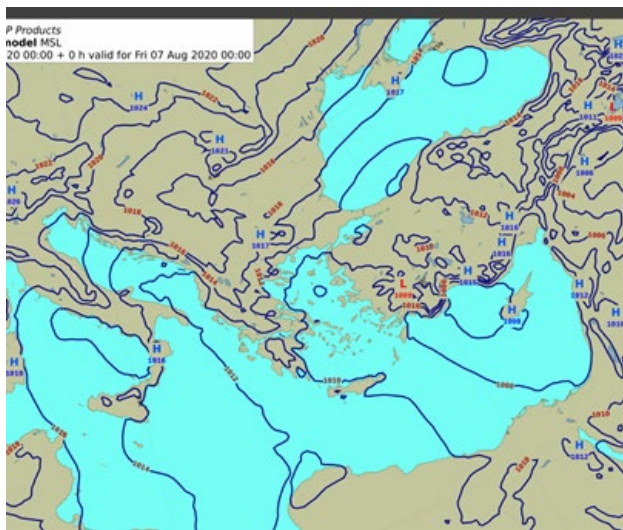
850hPa GH-T for 07/12UTC
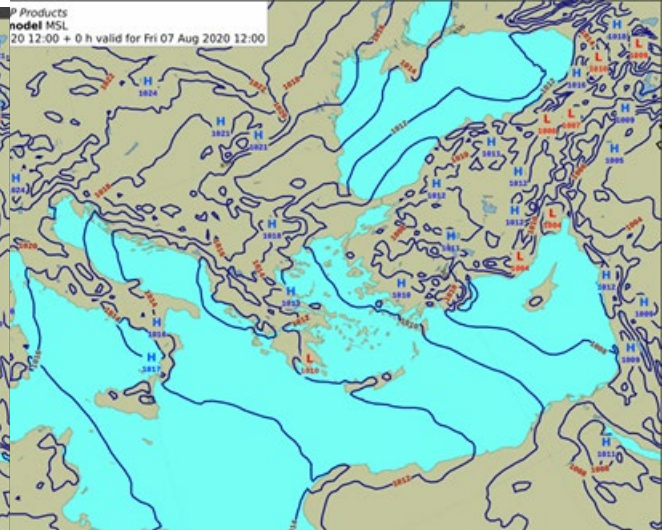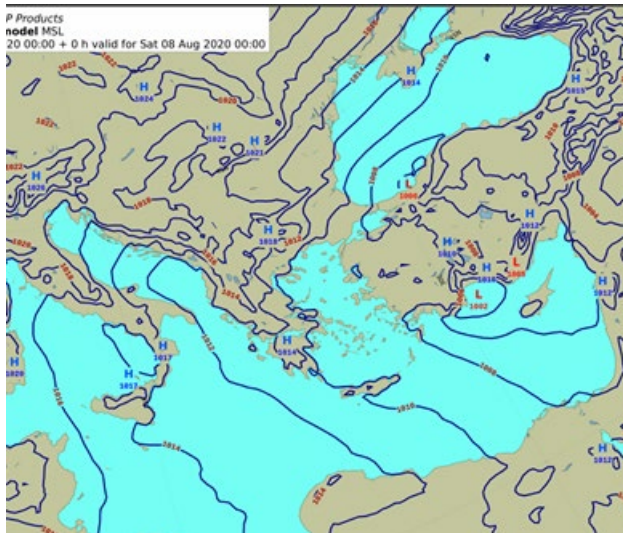
850hPa GH-T for 08/00UTC

850hPa GH-T for 08/12UTC

850hPa GH-T for 09/00UTC

MSLP for 07/00UTC

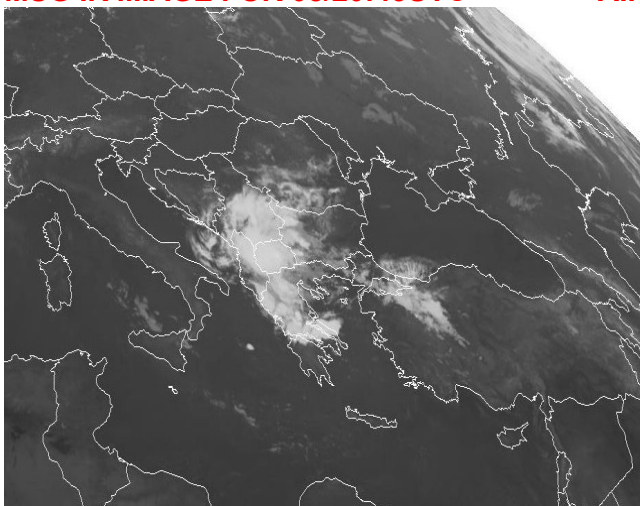**MSLP for 07/12UTC**

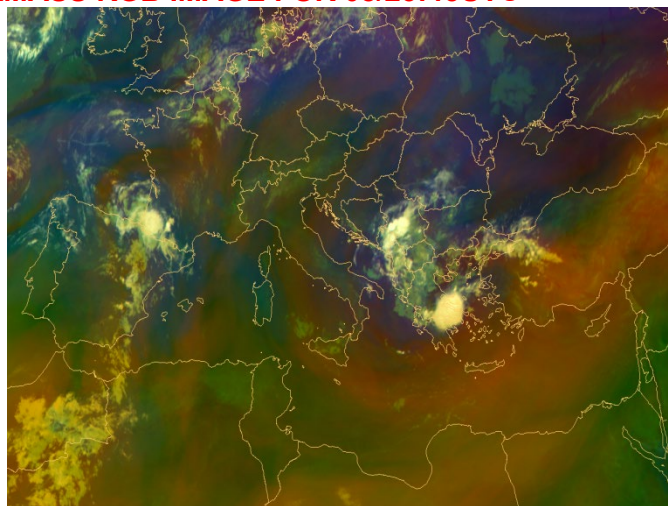**MSLP for 08/00UTC**

MSLP for 08/12UTC

MSLP for 09/00UTC

GREECE
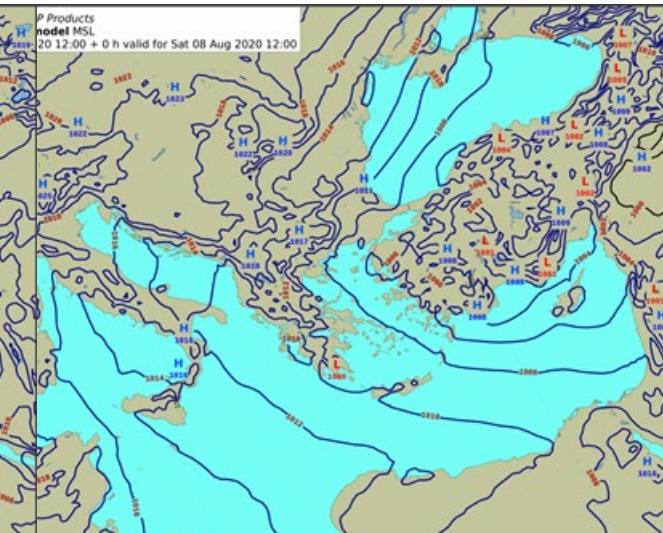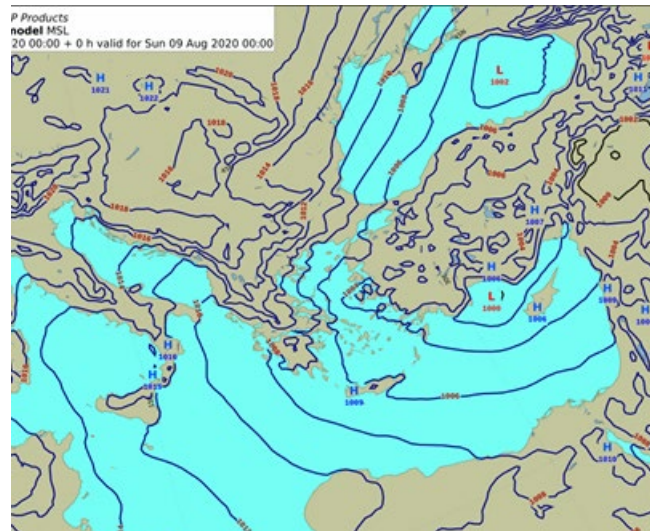
ECMWF 12HR TOTAL PRECIPITATION FORECAST   (09/00UTC – 09/12UTC)
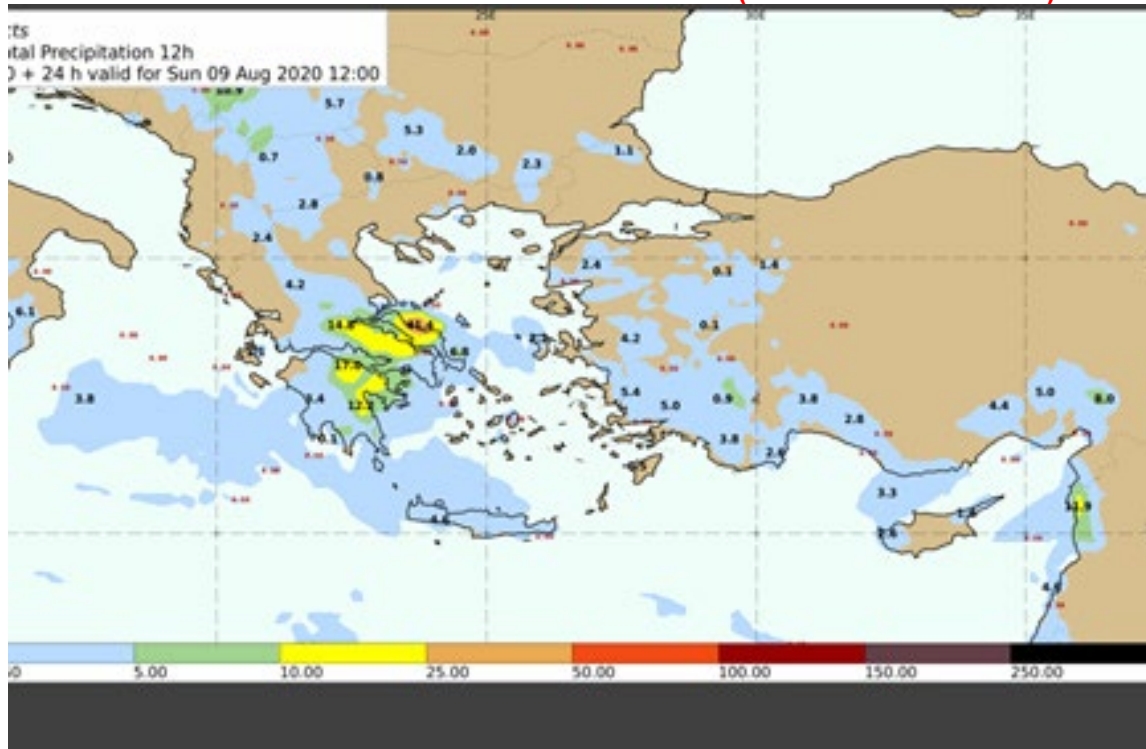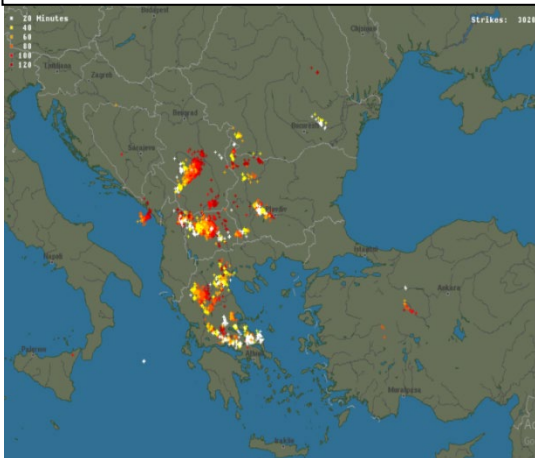

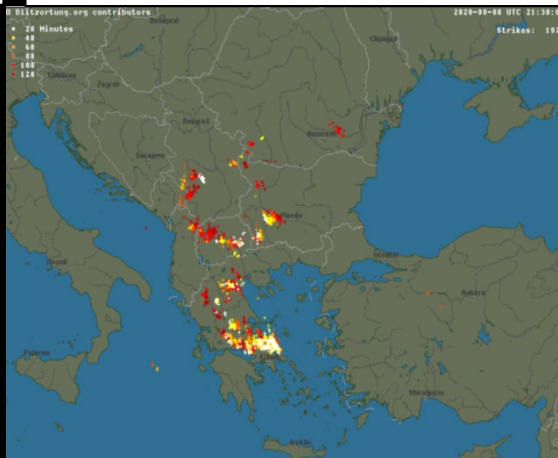**MSG IR IMAGE FOR 08/20:45UTC**
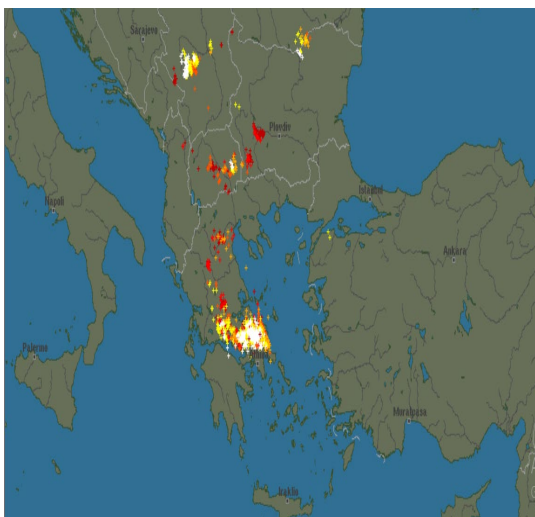
AIRMASS RGB IMAGE FOR 08/23:45UTC

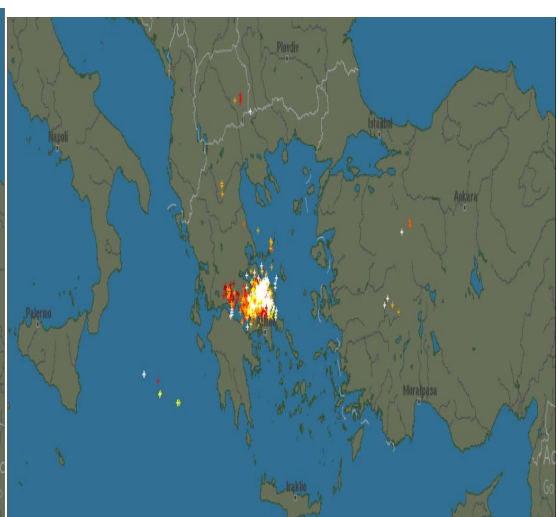**LIGHTINGS ACTIVITY FOR 08-08-2020 20:20UTC**

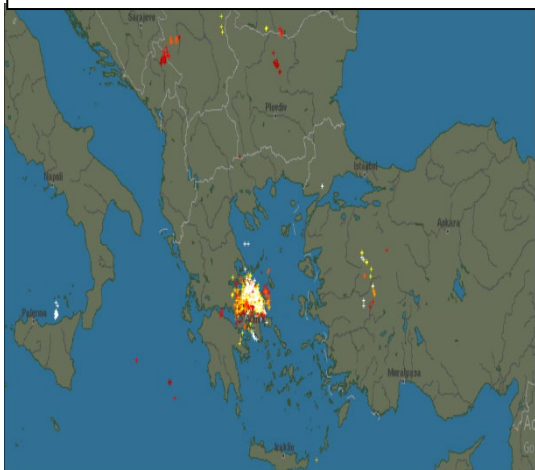**LIGHTINGS ACTIVITY FOR 08-08-2020 21:30UTC**
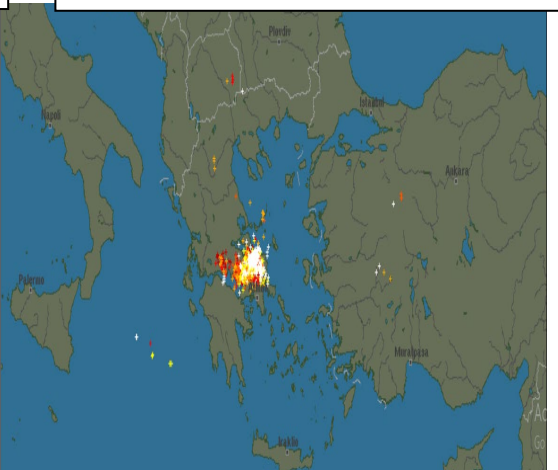
LIGHTINGS ACTIVITY FOR 08-08-2020 22:40UTC

LIGHTINGS ACTIVITY FOR 09-08-2020 00:35UTC

LIGHTINGS ACTIVITY FOR 09-08-2020 02:00UTC

LIGHTINGS ACTIVITY FOR 09-08-2020 05:00UTC

4.   References to relevant publications

Gofa, F., Boucouvala, D., Louka, P. and H Flocas , (2018) Spatial verification approaches as a tool to evaluate the performance of high resolution precipitation forecasts. *Atmospheric Research*, 208,, 78-87

Hart, R. E. (2003): A Cyclone Phase Space Derived from Thermal Wind and Thermal Asymmetry, *Monthly Weather Review*, *131*(4), 585-616

Hoskins, B. J.and Berrisford, P. (1988) A potential vorticity perspective on the storm of 15–16 October 1987. *Weather*, 43: 122–129

Prezerakos, N. G., and H. A. Flocas, (1996) The formation of a dynamically unstable ridge at 500 hPa as a precursor of surface cyclogenesis in the central Mediterranean. *Meteor. Appl*, **3 ,** 101–111.

Pytharoulis, I.; Kartsios, S.; Tegoulias, I.; Feidas, H.; Miglietta, M.M.; Matsangouras, I.; Karacostas, T.(2018) Sensitivity of a Mediterranean Tropical-Like Cyclone to Physical Parameterizations. *Atmosphere*, *9*, 436. https://doi.org/10.3390/atmos9110436

Shapiro M.A.and Keyser D. (1990) Fronts, Jet Streams and the Tropopause. In: Newton C.W., Holopainen E.O. (eds) Extratropical Cyclones. American Meteorological Society, Boston, MA. https://doi.org/10.1007/978-1-944970-33-8_10